nature reviews urology

https://doi.org/10.1038/s41585-022-00660-8

Review article

Check for updates

Microfluidics facilitating the use of small extracellular vesicles in innovative approaches to male infertility

Dale M. Goss[1,2], Steven A. Vasilescu[1,3], Gavin Sacks[2,4], David K. Gardner[5,6] ✉ & Majid E. Warkiani[1] ✉

Abstract

Sperm are transcriptionally and translationally quiescent and, therefore, rely on the seminal plasma microenvironment for function, survival and fertilization of the oocyte in the oviduct. The male reproductive system influences sperm function via the binding and fusion of secreted epididymal (epididymosomes) and prostatic (prostasomes) small extracellular vesicles (S-EVs) that facilitate the transfer of proteins, lipids and nucleic acids to sperm. Seminal plasma S-EVs have important roles in sperm maturation, immune and oxidative stress protection, capacitation, fertilization and endometrial implantation and receptivity. Supplementing asthenozoospermic samples with normospermic-derived S-EVs can improve sperm motility and S-EV microRNAs can be used to predict non-obstructive azoospermia. Thus, S-EV influence on sperm physiology might have both therapeutic and diagnostic potential; however, the isolation of pure populations of S-EVs from bodily fluids with current conventional methods presents a substantial hurdle. Many conventional techniques lack accuracy, effectiveness, and practicality; yet microfluidic technology has the potential to simplify and improve S-EV isolation and detection.

Sections

[1]School of Biomedical Engineering, University of Technology Sydney, Sydney, NSW, Australia. [2]IVF Australia, Sydney, NSW, Australia. [3]NeoGenix Biosciences pty ltd, Sydney, NSW, Australia. [4]University of New South Wales, Sydney, NSW, Australia. [5]Melbourne IVF, East Melbourne, VIC, Australia. [6]School of BioSciences, University of Melbourne, Melbourne, VIC, Australia. ✉e-mail: david.gardner@unimelb.edu.au; majid.warkiani@uts.edu.au

Key points

- Epididymosomes and prostasomes, the two distinct populations of seminal plasma small extracellular vesicles (S-EVs), have substantial roles in sperm function, survival and fertilization of the oocyte.
- Male reproductive S-EV protein and microRNA cargo might serve as biomarkers for infertility and reproductive dysfunction.
- Conventional methods of S-EV isolation require often laborious or costly workflows with suboptimal results but have received substantial interest in cancer therapeutics and diagnostics.
- Microfluidic technology has the potential for miniaturization and simplification of S-EV isolation and analysis for use in point-of-need diagnostics in male infertility.
- Infertility treatment can use technology developed for cancer diagnostics and therapeutics to approach idiopathic infertility.

Introduction

Nearly all cells in the body secrete at least one form of extracellular vesicle (EV) into the extracellular space in vivo and in vitro, with EVs having been observed circulating within all body fluids and perceived to be integral components of cellular communication in multicellular organisms[1–5]. These heterogenous, phospholipid bilayer-bound vesicles have garnered considerable attention, owing to their roles in intercellular communication to regulate normal function and disease states[6–9]. Advances in technology such as mass spectrometry, real-time quantitative PCR and nanoparticle tracking analysis (NTA) have helped to facilitate research into the highly complex and discrete molecular cargo exchanges between cells in nearly all systems within the body[6,10]. Evidence of EVs in biological fluids was first reported by Chargaff and West[11] in 1946, who analysed ultracentrifuged blood plasma using electron microscopy and described thromboplastic agents and blood corpuscles that sedimented after this centrifugation. The term 'extracellular vesicle' was not used until 1970, when Bonucci[12] observed calcifying properties of EVs in epiphyseal cartilage.

EVs can contain proteins, nucleic acids, lipids, metabolites and even organelles from parent cells, and range between 30 nm and 10 μm in size[13–15]. EVs are divided into three subgroups: small EVs (S-EVs; or exosomes); microvesicles (or ectosomes or large EVs); and apoptotic bodies (or apoptosomes), which differ in size, morphology, contents, biogenesis and secretion[10,16]. The subgroup nomenclature is specifically based on size and origin: S-EVs are 30–200 nm in size, spherical and are thought to originate from endocytosis; microvesicles are 100–1,000 nm in size, irregular in shape and are secreted by budding of the plasma membrane and shedding into the extracellular space; and apoptotic bodies are >1 μm in size,[13,17–20] produced by cells undergoing apoptosis and signal phagocytosis by macrophages[10]. Apoptotic bodies differ from other EVs in that they contain organelles, DNA fragments, partially degraded chromatin fragments, cytosolic portions and denatured proteins[18,21–23] (Fig. 1).

Seminal plasma was one of the first biofluids in which EVs were identified and observed[24] with S-EVs having been shown to contribute to the development, maturation and activation of sperm in the male and female reproductive tracts before and during fertilization[25–28]. S-EVs, as pivotal components of cell function, might, therefore, improve our understanding of basic function and dysfunction of both male and female reproductive systems. Several global proteomic and genomic approaches to identifying biomarkers within semen have been published, but no consensus has been reached on robust biomarkers linked to infertility and disease states; thus, seminal plasma S-EVs could have the potential to improve our understanding of idiopathic infertility and pathophysiological states, while providing novel approaches to both diagnostics and therapeutics in assisted reproductive technology (ART). Consequently, the isolation of pure populations of S-EVs is a step towards personalized reproductive medicine.

Conventional methods of S-EV isolation have many weaknesses including high costs, long processing times and low recovery and purity of S-EVs. These limitations remain a considerable hurdle in the progress of S-EV research and translation into clinical medicine. However, microfluidics, which is the multidisciplinary field of fluid manipulation and control within geometrically confined microchannels[29], has been applied to the separation of S-EVs in cancer research and diagnostics, in bladder[30], breast[31], liver[32], ovarian[33], pancreatic[34] and prostate[35,36] cancers. Microfluidic platforms require microlitre sample input volumes primarily using controlled micropumps for high purity isolation, low processing times and simple operation and, therefore, have the potential for routine application of S-EV isolation and analysis for diagnostics and therapeutics. Microfluidic geometry can also use and combine conventional approaches on one platform to isolate S-EVs, providing unique benefits such as reducing operational time, costs and manual steps, as well as enabling multiplex targeting of specific S-EVs in simplified workflows without the need for large and expensive equipment.

In this Review, we explore the diagnostic potential of male reproductive S-EVs and the practical approaches of implementing point-of-need and multianalyte diagnostics in infertility treatment, detailing microfluidic S-EV isolation and analysis as an accessible and effective approach to achieving this outcome, as well as proposing S-EV protein and microRNA (miRNA) biomarkers linked to various key events in sperm development, maturation and fertilization.

S-EVs and male reproduction

The role of S-EVs in male reproduction has been highlighted in studies in which the complex contribution of S-EVs to intercellular communication is explored in both normal healthy function and pathophysiological states, facilitating a broad array of physiological processes including cell proliferation, differentiation, gametogenesis, embryogenesis and development[37]. S-EV biogenesis, localization and transport within biofluids to target cells or tissues are imperative to understanding function within male reproduction and the downstream effects in which reproductive dysfunction can be identified and treated.

S-EV identification and biogenesis

S-EVs were first described in 1987 in a study in which vesicle formation during reticulocyte maturation in rat models was investigated[36]. Since then, a growing body of evidence has been supporting a correlative relationship between S-EVs and various physiological functions, disease states and diverse intercellular communication[38,39]. Importantly, S-EV cargo can reflect the physiological state of the donor cell, providing insight into cellular responses to the extracellular milieu as well as intercellular communication[40]. S-EV biogenesis begins with internalization of extracellular molecules via endocytosis, forming multivesicular bodies that sequester proteins, RNAs and lipids from the cytosol and

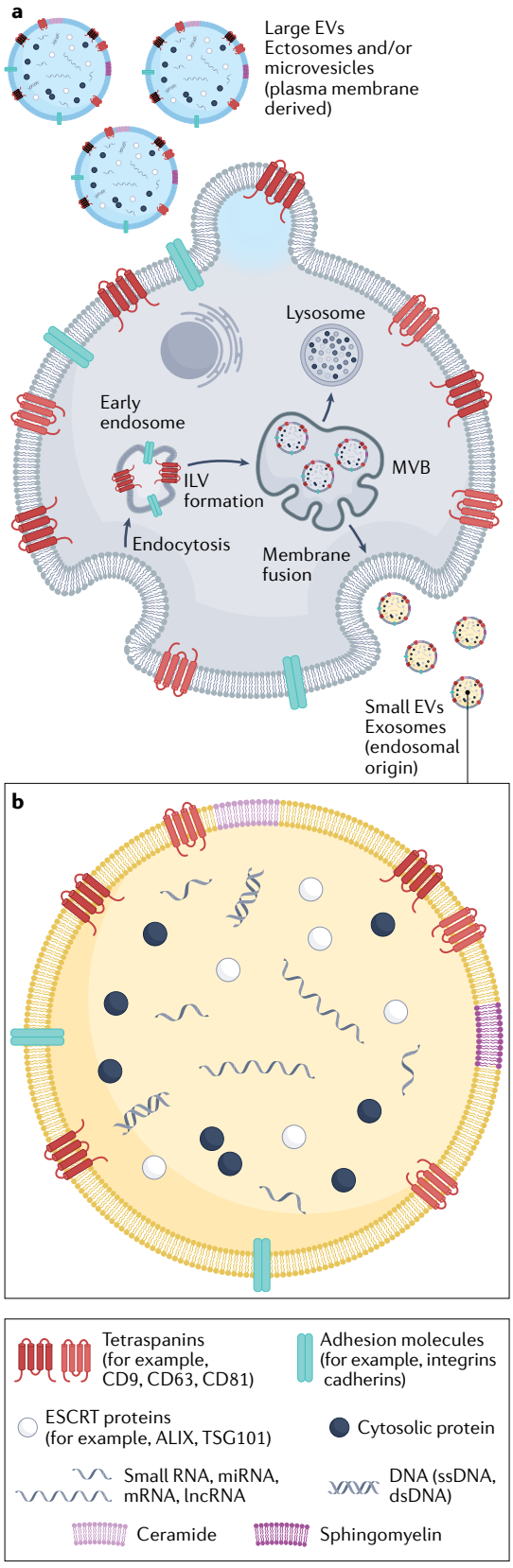

Fig. 1 | Biogenesis and release of EVs. a, Generation of extracellular vesicles (EVs). Small EVs (S-EVs, 50–150 nm) are formed by inward budding of late endocytotic intraluminal vesicles called multivesicular bodies (MVBs), which fuse with the plasma membrane to release the S-EVs into the extracellular space. Microvesicles and ectosomes (large EVs, 100–1,000 nm) are secreted by budding from the plasma membrane. **b**, S-EV structure and cargo. S-EVs are characterized by specific surface markers such as tetraspanins, endosomal sorting complex required for transport (ESCRT) proteins and adhesion molecules, and contain nucleic acids (RNAs and DNA), as well as proteins. ALIX, ALG2-interacting protein X; dsDNA, double-stranded DNA; ILV, intraluminal vesicle; lncRNA, long non-coding RNA; miRNA, microRNA; ssDNA, single-stranded DNA. Adapted from ref.[371], Springer Nature Limited.

trans-Golgi network to form intraluminal vesicles by inward budding of the endosomal membrane[10,41]. These intraluminal vesicles are then secreted into the extracellular space as S-EVs via exocytosis when the multivesicular and plasma membranes fuse[17] (Fig. 1).

S-EVs are subsequently released into the extracellular space to mediate intercellular communication via transportation of genetic material such as mRNA and miRNA, as well as proteins and lipids between cells both locally (autocrine and paracrine) and remotely, and can facilitate interaction between cells, both independently and in collaboration with growth factors and hormones[42–44]. Whether S-EVs function as single entities or in unison as aggregates with a common target is yet to be established owing to the challenging nature of S-EV isolation[34]. Emphasis has been placed on the potential of S-EVs as diagnostic biomarkers or therapeutic agents for research into disease states[45] such as cancer[39,46,47], neurodegenerative diseases[48,49], immune responses to viral infections[50,51], and both male and female infertility[52–54].

S-EVs in seminal plasma

Fertility treatment is an evolving field with a high demand for improvement; therefore, innovation in understanding both the often idiopathic nature of infertility and the treatment approaches is urgently required. Seminal plasma has been shown to contain high concentrations of S-EVs originating from the prostate and epididymis, accounting for the large majority of identifiable S-EV proteins and cargo found in seminal plasma[55,56]. Seminal plasma S-EVs were first described by Ronquist and Hedström[57] in 1977 who analysed human prostatic fluid using electron microscopy; these prostatic EVs were later termed ‘prostasomes’ in studies published by the same group in 1983 (ref.[58]) and 1985 (ref.[59]) based on their origin; however, historically, the term prostasome has been used to refer to all S-EVs found in seminal plasma[24,60–62]. Subsequently, S-EVs from the epididymis were discovered in humans and aptly named ‘epididymosomes’, and the conclusion was made that multiple components of the male reproductive system were secreting vesicles into seminal plasma[63–65]. EVs from bovine seminal vesicles have also been identified and shown to present with similar morphology to both prostasomes and epididymosomes, although at lower concentrations in ejaculated semen[66]. However, EVs from seminal vesicles are difficult to isolate and study, as no proteins expressed exclusively by the seminal vesicles[67], or surface markers and morphological differences in prostasomes, have been identified[64]. Seminal vesicles in humans primarily contribute fructose[68], prostaglandins[69] and semenogelins[70] and little research into S-EV-mediated signalling or protein transfer to sperm has been conducted.

Seminal plasma S-EVs are particularly important as sperm are transcriptionally and translationally quiescent owing to DNA packaging

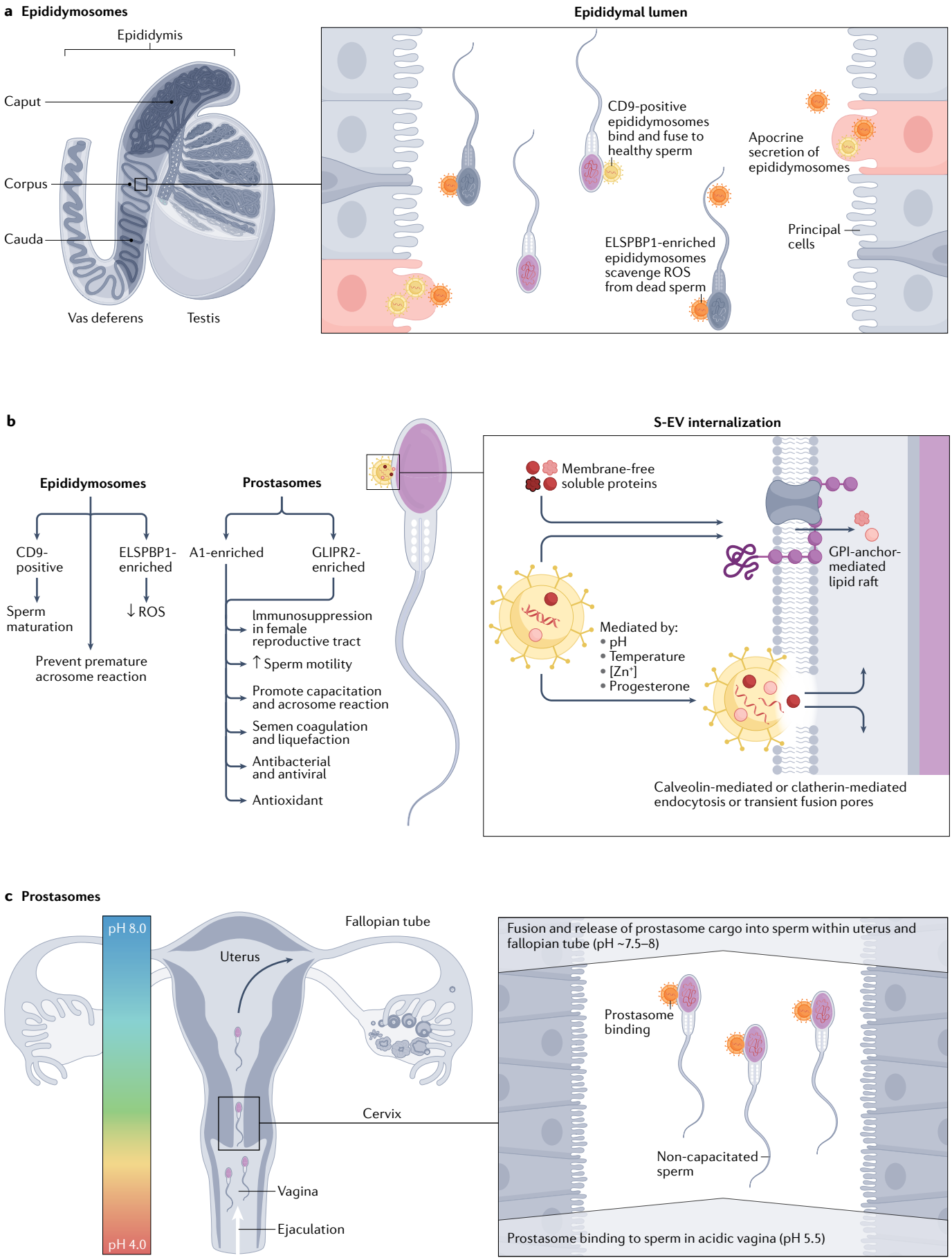
a Epididymosomes
Epididymis
Caput
Corpus
Cauda
Vas deferens
Testis
Epididymal lumen
CD9-positive epididymosomes bind and fuse to healthy sperm
Apocrine secretion of epididymosomes
ELSPBP1-enriched epididymosomes scavenge ROS from dead sperm
Principal cells
b
Epididymosomes
CD9-positive
ELSPBP1-enriched
Sperm maturation
↓ ROS
Prevent premature acrosome reaction
Prostasomes
A1-enriched
GLIPR2-enriched
Immunosuppression in female reproductive tract
↑ Sperm motility
Promote capacitation and acrosome reaction
Semen coagulation and liquefaction
Antibacterial and antiviral
Antioxidant
S-EV internalization
Membrane-free soluble proteins
GPI-anchor-mediated lipid raft
Mediated by:
• pH
• Temperature
• [Zn+]
• Progesterone
Calveolin-mediated or clatherin-mediated endocytosis or transient fusion pores
c Prostasomes
pH 8.0
pH 4.0
Uterus
Fallopian tube
Cervix
Vagina
Ejaculation
Fusion and release of prostasome cargo into sperm within uterus and fallopian tube (pH ~7.5–8)
Prostasome binding
Non-capacitated sperm
Prostasome binding to sperm in acidic vagina (pH 5.5)

Fig. 2 | Male reproductive S-EVs from the epididymis and prostate and their roles in sperm maturation, protection and interaction with the oocyte. **a**, Epididymosomes are secreted by principal cells of epididymal lumen in an apocrine manner. CD9-positive small extracellular vesicles (S-EVs) are involved in protein transfer to immotile epididymal sperm leaving the testes, which facilitates sperm maturation and ELSPBP1-enriched epididymosomes bind to dead and dying sperm and are believed to reduce reactive oxygen species (ROS) levels. **b**, Binding and fusion of epididymosomes and prostasomes occurs by different mechanisms, either by glycosylphosphatidylinositol (GPI)-anchor-mediated lipid raft protein transfer or via formation of transient fusion pores. **c**, Prostasomes are released into the acinar lumen of the prostate and bind to sperm in the acidic vagina and fuse once the pH neutralizes through the cervix, promoting capacitation. Binding occurs either at the acrosomal cap or neck and midpiece[17].

from histones to protamines; thus, post-testicular maturation events in the epididymis and female reproductive tract need to be facilitated through external signals such as S-EVs and soluble signalling molecules[60,71–74]. Seminal plasma S-EV binding, fusion and cargo delivery to sperm occurs both in the epididymis and post-ejaculation in the female reproductive tract[25]. This revelation highlighted the receptiveness of sperm to S-EV binding in the vaginal canal and the role prostasomes have in capacitation and fertilizing capacity based on the sperm's localization within the female reproductive tract. The importance of seminal plasma EVs not only in fertilization, but also in embryo implantation and reproductive outcomes has been supported by in vitro evidence showing that seminal plasma S-EVs enhance in vitro endometrial stromal cell decidualization and increase secretion of prolactin, an essential hormone in implantation[75], and regulate porcine endometrial epithelial cell gene expression linked to immune and inflammatory responses, as well as steroid biosynthesis[76]. Embryo implantation was shown to be ~40% lower in mice after intrauterine perfusion of seminal plasma from old males than seminal plasma from young males[77]. Furthermore, this reduction in implantation rate was partially rescued by supplementing old male seminal plasma with young seminal plasma S-EVs before pre-implantation intrauterine perfusion, with an increase of 20%[77]. These differences were attributed to variations in S-EV contents from the old and young males causing immunomodulation of endometrial cells via cytokine and chemokine expression[77].

A re-evaluation of the protein contents and linked functions of seminal plasma EVs showed three distinct populations of EVs based on relative density — namely, high-density, medium-density and low-density vesicles — along with non-vesicular extracellular matter[70]. High-density EVs and non-vesicular extracellular matter could promote sperm motility and capacitation, whereas medium-density EVs might reduce intrinsic reactive oxygen species (ROS) in sperm, indicating the functional and structural heterogeneity of seminal plasma S-EVs (Fig. 2), which have various forms of interaction with sperm throughout the male reproductive system and post-ejaculation.

Epididymosomes. Epididymosomes were first identified in 1985 and described as cholesterol-rich microvesicles in close-contact with sperm within the hamster epididymal lumen, and were hypothesized to be involved in sperm maturation and membrane stabilization[78]. These vesicles have since been described in epididymal fluid from humans[79], cows[80,81], mice[82,83], sheep[84,85] and rats[86,87]. Once sperm leave the testes, they migrate through the three segments of the highly convoluted epididymis, beginning at the proximal caput, moving through the central, elongated corpus and finally into the distal cauda (Fig. 2a). These segments are distinct in regional gene and protein expression and the caput epididymis has presented with the most abundant and diverse secretome, whereby testicular proteins are rapidly absorbed and epididymal proteins are secreted to begin the series of biochemical changes sperm undergo through the epididymis, giving sperm the ability to fertilize the oocyte[79,88–92]. Gene and protein expression differences coincide with epididymal epithelial cell morphology and functional changes as sperm lose cytosolic organelles during transit through the epididymal lumen, as well as the loss or modification of testicular surface proteins and acquisition new proteins and lipids obtained within the epididymis via epididymosomes, direct transfer or associated with binding proteins such as clusterin and lipocalins[81,93–95]. Heterogeneity in the size and content of epididymosomes is also evident throughout the segments of the epididymis[96,97] and release of these proteins and lipids from the epididymal epithelium is regulated by testicular androgens and other poorly understood factors such as luminal pH[82], intratubular pressure[98] and intraluminal flow[63,99]. Robust human studies into epididymal sperm and the epididymal microenvironment are limited owing to poor access to epididymal sperm and fluid devoid of contributions from the prostate and bulbourethral glands. Thus, with most prominent research on epididymosomes and epididymal sperm being performed on animal models and results showing species-specific epididymal secretomes, assumptions regarding specific biomarkers in humans should be approached with care and rigorous validation[100].

Epididymosomes constitute a relatively small proportion of S-EVs in ejaculated semen, indicating that a large part of their function occurs during epididymal transit[55]. Epididymosomes range from 25 nm to 300 nm in size and have membranes containing cholesterol-concentrated and sphingomyelin-concentrated lipid rafts that are important for protein transfer between epididymosomes and sperm, which has been demonstrated in both bull[101] and mouse[102] models. These lipid rafts are present on the plasma membranes of nearly all mammalian cells and have a well-described mechanism of signalling via protein and lipid trafficking, suggesting conserved mechanisms of S-EV interaction with mammalian cells[103,104]. Immotile differentiated sperm departing the testes lack fecundity and gain these traits during maturation, largely facilitated by S-EV-bound proteins released by pseudo-stratified epididymal epithelium in an apocrine manner[82,105]. The predominant, widely accepted method of protein and signal transfer in the mammalian epididymis is facilitated by S-EVs, although soluble proteins within epididymal luminal fluid have been shown to enter sperm via non-vesicular processes[106,107].

Epididymosomes are believed to consist of two distinct subgroups: epididymal sperm binding protein 1 (ELSPBP1)-enriched epididymosomes and CD9-positive epididymosomes, according to bovine studies[108–110] (Fig. 1b). ELSPBP1-enriched epididymosomes are thought to protect epididymal sperm from oxidative damage by forming a complex with biliverdin reductase A (BLVRA) and binding to dead and dying sperm, reducing biliverdin to bilirubin using NADPH, which can sequester ROS to convert bilirubin back to biliverdin, in the presence of Zn^{2+} (refs.[111,112]). CD9-positive epididymosomes bind and fuse with sperm in a temperature-dependent and pH-dependent manner during transit through the epididymis and are believed to promote mammalian sperm maturation events, such as Ca^{2+} membrane channel regulation[113], sperm–zona pellucida (ZP) binding capacity[114], motility acquisition[115] and prevention of premature acrosome reaction, via transfer of proteins to the post-acrosomal sheath and midpiece[81,88,116]. This binding and protein transfer occurs via glycosylphosphatidylinositol (GPI)-anchor-mediated docking in a highly selective manner[90,117] (Fig. 2b). The process of epididymal sperm maturation comprises several substantial physiological changes to sperm, mediated in

part by epididymosome transfer of proteins and lipids to maturing sperm[118]. These changes have been identified in human, mouse, rat and bull models and include increasing levels of sphingomyelin while decreasing cholesterol content from the caput to cauda[119], reducing sperm membrane rigidity[82,119], increasing total negative charges on the sperm surface[120,121], relocalization of sperm surface antigens[122,123], increasing disulphide bonds[124] and removal, addition and modification of surface proteins[125,126].

Prostasomes. Prostasomes are bilamellar to multilamellar membrane-bound vesicles measuring 30–500 nm that are released into the acinar lumen of prostate epithelial cells and constitute most seminal plasma S-EVs[127]. Unlike the apical blebbing of epididymosomes, prostasomes are believed to require membrane fusion of multivesicular bodies to the epithelial membrane to be released into prostatic fluid[128,129]. EVs in seminal plasma were first identified in semen; these EVs were of prostatic origin and, therefore, the term 'prostasomes' was used as the nomenclature for all EVs found in seminal plasma[130]; however, here, this term is used exclusively for S-EVs secreted by the prostate. In contrast to epididymosomes, acquiring human semen samples rich in prostatic secretions is relatively simple and the role of prostasomes in sperm physiology[131] and possible biomarkers in prostasome cargo[88] have been extensively explored.

As with epididymosomes, two discrete populations of prostasomes exist, depending on size and molecular composition: small, glioma pathogenesis-related 2 (GLIPR2)-enriched prostasomes and large, annexin A1 (ANXA1)-enriched prostasomes, as shown in vasectomized men and stallions[28,132] (Fig. 2b). No functional differentiation has been conducted between the two identified populations of prostasomes. Human studies have shown that prostasomes contain an assortment of important molecules including enzymes, signalling proteins, cellular chaperone proteins, transport and structural proteins and GTP-binding proteins[55,61,88]. Several important prostate-specific proteins have been identified in prostasome cargo including prostate acid phosphatase (PAP), prostate-specific antigen (PSA), type 2 transmembrane serine protease (TMPPRSS2), prostate-specific transglutaminase (pTGase) and prostate stem cell antigen (PSCA)[55,61]. Prostasomes have a pivotal role in sperm motility and regulation of sperm acrosome reaction timing, executed through to transfer of Ca^{2+} signalling receptors to the neck of ejaculated sperm[27]. Once sperm reach the lower portion of the female reproductive tract, prostasomes are postulated to loosely bind or 'piggy-back' onto sperm in the acidic environment of the vagina (~pH 5.0) and be carried into the uterus and oviduct where binding occurs in the presence of bicarbonate at pH 7.5–8.0 and subsequent fusion and transfer of prostasome contents into sperm at more alkaline conditions of the uterus and oviduct before fertilization[133,134] (Fig. 2c). During migration through the vagina, cervix, uterus and oviduct, prostasome fusion transfers proteins, lipids and RNAs that promote ZP binding capacity, acrosome reaction priming and hyperactive motility before interaction with the cumulus oocyte complex (COC)[130,134] (Fig. 2c). Specifically, prostasome fusion transports progesterone receptors, cyclic adenosine diphosphoribose (cADPR)-synthesizing enzymes and ryanodine receptors (RyRs) to sperm, which leads to increases in Ca^{2+} in sperm, which is responsible for flagellar motility and ultimately fertilization[27,135]. Prostasomes also influence capacitation by increasing intracellular cAMP, stimulating protein kinase A (PKA) to induce tyrosine phosphorylation[136–139]. Furthermore, sperm are well-documented to be immunologically identified as foreign bodies by the female reproductive tract immune cells; consequently, prostasome interactions in the female reproductive tract locally regulate female immunological responses to sperm by inhibiting monocyte and neutrophil phagocytosis and natural killer (NK) cell activity[140,141]. This inhibition is achieved by rapid binding of prostasomes to the female immune cell membranes and transfer of immuno-regulatory miRNA biotypes and proteins via endocytosis[142]. Prostasome immunosuppressive activity has been repeatedly corroborated in humans and animal models by the observed immune responses in the vaginal canal and uterus when isolated and washed sperm are administered, when compared with a lack of immune response to whole semen[143–145].

Prostasomes as a target for point-of-care tests have been used in prostate cancer diagnostics, with several research groups developing diagnostic platforms to isolate prostasomes and prostatic tumour S-EVs to identify and characterize cancer-specific proteins[35,36] and miRNA[30] biomarkers for early detection[146].

Notable seminal plasma S-EV proteins

Seminal plasma is composed of secretions from the epididymis, seminal vesicles, prostate and bulbourethral glands and contains a vast array of proteins found within S-EVs and EVs[147]. Seminal plasma S-EVs contain only 3% of total seminal plasma protein, but, owing to their unique regulatory functions and reflection of the status and health of their parent cell, S-EV proteins have considerable biomarker potential for diagnosis or prognosis in male reproductive pathological conditions and infertility[56,119]. Furthermore, S-EVs preserve their contents by isolating these proteins and nucleic acids from deleterious factors such as enzymes (proteases and RNases), ROS and environmental factors that probably cause degradation[148]. Protein transfer between seminal plasma S-EVs and sperm has been attributed to overall sperm function[149], maturation[97], morphology[150], acquisition and maintenance of motility[26], concentration[151] and protection from oxidative damage[152,153]. Generally, S-EV protein composition varies drastically, but, owing to common methods of biogenesis, most S-EVs express common surface markers such as tetraspanins, which are organizing scaffold proteins constituting plasma membrane microdomains, containing adhesion, adaptor and signalling proteins, aiding in the identification and characterization of S-EV populations once isolated[154].

Purification of S-EVs from seminal plasma has enabled identification of vast protein content profiles specific to seminal plasma S-EVs using global proteomic studies. For example, 1,474 seminal plasma S-EV proteins were identified in samples from men with normospermia[137] and 1,282 proteins from prostasomes were identified from both men with normospermia and those with non-normospermia[138]; furthermore, proteins involved in sperm energy production and activity were found to be downregulated in non-normospermic men.

The protein composition of seminal plasma S-EVs varies greatly depending on origin and proposed function. For example, CD9-positive epididymosomes are enriched with P25b, GliPr1L1 and MIF, which are all known as important proteins in sperm motility and gain of the ability to recognize the oocyte and interact during fertilization[109,155]. Prostasomes contain a discrete protein profile based on the initiation of hypermotility, capacitation and acrosome reaction once sperm reach the female reproductive tract and ultimately the cumulus oocyte complex[60,131,156]. Well-categorized proteins such as PAP, PSA, pTGase, PSCA, TMPRSS2 and CD48 have been strongly associated with prostasomes and largely thought to be involved in Ca^{2+} concentration and pH regulation within sperm, regulating sperm motility, capacitation, acrosome reaction and the female reproductive tract immune response[27,55,136,157]. Prostasome

Table 1 | Male reproductive S-EV proteins of interest[a]

Accession number	Protein name	Gene	S-EV source	Function in male fertility	Refs.
P54107	Cysteine-rich secretory protein 1	*CRISP1*	Epididymosomes and prostasomes	Sperm–ZP binding Decapacitation factor Regulation of $Ca2^+$ ion channels (hypermotility and fertilization)	63,113,159–162,164,165,329
P07864	L-Lactate dehydrogenase C chain	*LDHC*	Prostasomes	Sperm energy metabolism (anaerobic glycolysis) Sperm motility Fertilization	159,167,168,172,330–332
P14174	Macrophage migration inhibitory factor	*MIF*	Epididymosomes and prostasomes	Sperm maturation and motility (sperm-dense fibres) Positive association with DFI and reduced motility Spermatogonia cell migration High levels linked to endometriosis-linked infertility	101,115,159,174,175,177–179,333
Q7Z4W1	L-Xylulose reductase (P34H)	*DCXR*	Epididymosomes	Sperm–ZP binding and fertilization	180–187
Q9H2U9	Disintegrin and metalloproteinase domain-containing protein 7	*ADAM7*	Epididymosomes	Sperm–oocyte plasma membrane adhesion and fusion during fertilization Sperm migration through female reproductive tract Sperm maturation	188,189,334–336
P12273	NPC intracellular cholesterol transporter 2	*NPC2*	Epididymosomes and prostasomes	Sperm membrane stabilization and fertilization ability	55,63,122,190–192, 194,337,338
O75715	Epididymal secretory glutathione peroxidase	*GPX5*	Epididymosomes	Phospholipid hydroperoxidase (maintains cell and DNA integrity by protecting sperm from oxidative stress Might prevent premature acrosome reaction	82,153,192,197,198,339
P38567	Sperm adhesion molecule 1	*SPAM1*	Epididymosomes	Cumulus penetration Sperm–ZP adhesion Sperm maturation and storage	83,114,201,203,204,340–342
Q99497	Parkinson disease protein 7	*PARK7*	Epididymosomes	Protection from oxidative stress Spermatogenesis Fertilization	63,205,207–210,343,344

DFI, DNA fragmentation index; S-EV, small extracellular vesicle; ZP, zona-pellucida. [a]Listed in order of those with the most biomarker potential to the least.

surface proteins such as annexins I, II, IV, V, VII and XI are also believed to be regulators of Ca^{2+} concentration within sperm, therefore, affecting motility[61,158]. Clinically relevant evidence shows the important role that notable proteins have (Table 1, Fig. 3).

Cysteine-rich secretory protein 1. Cysteine-rich secretory protein 1 (CRISP1) is part of the CRISP, antigen 5 and pathogenesis related protein 1 (CAP) superfamily of proteins and is highly conserved and enriched in the mammalian reproductive tract, having been identified in both secreted epididymosomes and prostasomes[63,159]. CRISP1 modulates CatSper, the primary Ca^{2+} channel in sperm, which is essential in hyperactivation and fertilization[160] (Fig. 3). Studies in rat models have identified CRISP1 as a possible de-capacitation factor[161–163], and recombinant human CRISP1 negatively competes with zona pellucida sperm-binding protein 3 (ZP3), preventing sperm–ZP binding, penetration and subsequent fertilization[164,165]. Furthermore, *Crisp1* double-knockout mice produced sperm with impaired ZP-binding, and CRISP1 supplementation can improve pre-capacitation progressive motility[113]. The relative content of prostasomal CRISP1 is reduced in men with non-normospermia[138] and considerably reduced levels of CRISP1 have been observed in S-EVs from men with azoospermia compared with fertile men with normospermia[68] (Table 1, Fig. 3). CRISP1 has the potential to be used as a biomarker of both sperm capacitation ability as well as sperm–ZP binding capacity, which could indicate bypassing conventional sperm–oocyte interaction in conventional in vitro fertilization (IVF) and opting for intracytoplasmic sperm injection (ICSI).

L-Lactate dehydrogenase C chain. L-Lactate dehydrogenase C chain (LDHC) is a glycolytic enzyme that is found in both epididymosomes and prostasomes and is involved in the development of sperm and the production of ATP to fuel flagellar movement and capacitation[166] (Fig. 3). Lactate dehydrogenase (LDH) enzymes catalyse the conversion of pyruvate to lactate through the oxidation of NADH to NAD^+ (ref.[167]). LDHC has been shown to be highly expressed in testicular germ cells and sperm[168,169] and inhibition of LDH in both murine and bovine sperm has been shown to suppress capacitation[170,171]. Disruption of the *Ldhc* gene in mice caused severe infertility owing to the impairment of progressive motility, hypermotility and cellular ATP production[172]. LDHC content has also been shown to be reduced in prostasomes from men with non-normospermia[63,159] (Table 1). LDHC has biomarker potential for sperm motility dysfunction forming part of important capacitation events before fertilization, indicating the method of fertilization (IVF or ICSI) that would provide improved results.

Macrophage migration inhibitory factor. Macrophage migration inhibitory factor (MIF) is a ubiquitous, multifunctional pro-inflammatory cytokine with noted roles in innate immune response and inflammation[173] and Leydig cell regulation of Sertoli cell inhibin production[174]. The role of MIF in sperm physiology remains unclear, but it has been identified in both epididymosomes and prostasomes and is released by primary Sertoli cells, suggesting roles in sperm maturation in the epididymis, fertilization and spermatogonial migration, respectively[61,175,176]. MIF has been observed to concentrate in dense fibres of the epididymal sperm flagellar and regulating zinc content, implying

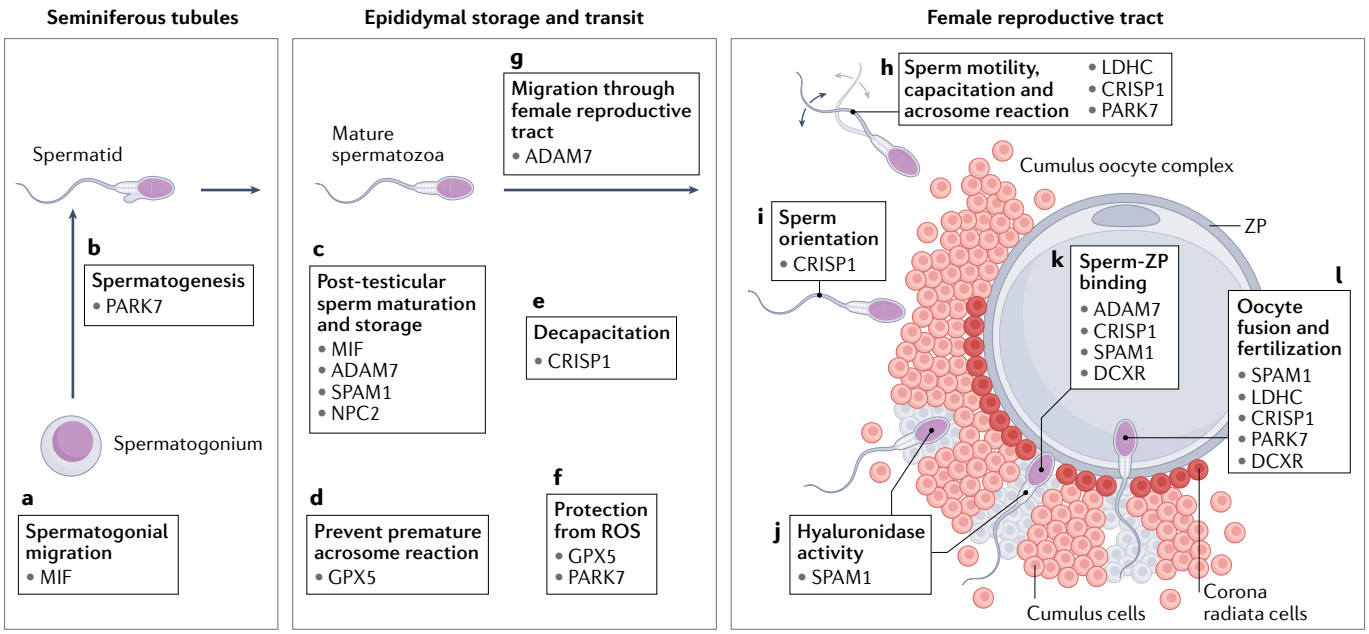

Fig. 3 | Potential seminal plasma small extracellular vesicle protein biomarkers and their involvement in key events during sperm development and function. a, Spermatogonial migration for survival, fate maintenance and differentiation of germ cells. **b**, Spermatogenesis, transforming spermatogonia into mature spermatozoa. **c**, Post-testicular maturation of sperm within the epididymis comprises membrane lipid remodelling and dynamics for storage while preparing for capacitation. **d**, Preventing premature acrosome reaction during storage and epididymal transit. **e**, Decapacitation is a reversible process preventing spontaneous initiation of capacitation signalling cascades. **f**, Protection from reactive oxygen species (ROS) and subsequent oxidative stress caused by environmental factors and dead or dying sperm within the epididymis. **g**, Female reproductive tract migration enabled by the motility and boundary-following tendency of ejaculated sperm. **h**, Sperm motility, capacitation and AR enable navigation through the oviduct, hyperactivation and furrowing through cumulus cells to the zona pellucida (ZP). **i**, Sperm orientation is modulated by hyperactivation and enables sperm to furrow through the cumulus cell complex. **j**, Hyaluronidase enzymes are released by the acrosome to digest hyaluronan in the cumulus extracellular matrix and corona radiata, enabling access to the ZP. **k**, Sperm–ZP binding occurs once the acrosome reaction has caused the release of enzymes and surface antigens permitting fusion of the sperm plasma membrane with the ZP. **l**, Oocyte fusion and fertilization involves the sperm plasma membrane and the oolemma and releasing of the sperm pronucleus for fusion with the oocyte pronucleus.

a possible role for MIF in sperm motility and the observed negative relationship with seminal plasma zinc concentration[115,177] (Fig. 3). Furthermore, the observed amount of sperm-associated MIF has a negative correlation with sperm motility and sperm DNA fragmentation index (DFI)[178,179]. Thus, MIF has a role in sperm development and maturation, and might inhibit sperm motility during epididymal migration and storage (Table 1). MIF has the potential to be used as a biomarker for sperm DFI and both testicular and epididymal sperm maturation.

Dicarbonyl/L-xylulose reductase. Dicarbonyl/L-xylulose reductase (DCXR; also known as P34H), is a multifunctional protein involved in monosaccharide catabolism, carbonyl detoxification, cell adhesion and male fertility that has been identified in epididymosomes in the corpus region of the epididymis[180,181]. The orthologue of DCXR in hamsters (P26H) has been shown to facilitate sperm–ZP binding[182] and reduced levels of the DCXR orthologue P25b in bulls correlated with subfertility[183]. Furthermore, reduced seminal DCXR content correlated with infertility and impaired ZP-binding capacity when comparing men with infertility with a fertile population as well as cycle failures in IVF treatment[184–186] (Fig. 3). DCXR has been proposed as a predictive marker of IVF success and might aid in the prediction of sperm maturation status before fertilization[186,187] (Table 1).

Disintegrin and metalloproteinase domain-containing protein 7. Disintegrin and metalloproteinase domain-containing protein 7 (ADAM7) is an important sperm membrane protein that is transferred directly to sperm through epididymosomes within the epididymis[188]. An ADAM7 protein complex is considerably promoted during capacitation events, forming a chaperone complex that is believed to contribute to the fertilization capacity of sperm in mice[189] (Fig. 3). Results of other mice studies showed that *Adam7*-knockout mice present with impaired sperm motility, morphology and disruption of important membrane proteins ITM2B and ADAM2 (ref.[174]). Results of studies using human samples have corroborated this observation by showing that reduced content of ADAM7 in seminal plasma S-EVs is associated with the presence of asthenozoospermia[26] (Table 1). Thus, ADAM7 has the potential to be used as a biomarker of epididymal sperm maturation, sperm migration through the female reproductive tract in natural conception as well as intrauterine insemination and the sperm–oocyte interaction.

NPC intracellular cholesterol transporter 2. NPC intracellular cholesterol transporter 2 (NPC2; also known as HE1) is an important cholesterol-binding protein secreted primarily in the epididymis and found in both epididymosomes and prostasomes[63,122]. NPC2 is thought to regulate epididymal sperm membrane cholesterol:phospholipid

molar ratios during maturation in humans[190], mice[191] and pigs[192,193] (Fig. 3). Seminal plasma NPC2 content is considerably down-regulated in oligoasthenozoospermia and vasectomized men have reduced epididymal NPC2 expression, resulting in impaired sperm with abnormally high cholesterol content[190,194]. Sperm from *Npc2*-knockout mice have reduced fertilizing ability and impaired energy metabolism linked to hyperactivation[191]. NPC2 as an epididymosome or prostasome protein marker has the potential to be an indicator of complete membrane-based sperm maturation and a functional epididymal environment (Table 1).

Epididymal secretory glutathione peroxidase. Epididymal secretory glutathione peroxidase (GPX5) is an isoenzyme with glutathione peroxidase activity secreted into the epididymis inside epididymosomes as free soluble proteins or bound to sperm membranes, functions in collaboration with GPX2 to protect sperm from lipid peroxidation and prevents premature acrosome reaction in the epididymis[153,192,195–197] (Fig. 3). *Gpx5*-knockout mice models show increased levels of oxidative stress in the testes, resulting in increased miscarriage and offspring mortality owing to developmental abnormalities in the embryos produced[153]. A positive relationship between seminal plasma GPX5 and both sperm quality and artificial insemination outcome in pigs has been observed[198]. GPX5 content in epididymosomes has the potential to reflect the antioxidant capacity of the epididymal lumen and protection of sperm during storage and migration through the epididymis (Table 1).

Sperm adhesion molecule 1. Sperm adhesion molecule 1 (SPAM1, or hyaluronidase PH-20) is a hyaluronidase enzyme found GPI-anchored on plasma membranes of both acrosome-intact and acrosome-reacted sperm heads[199,200], and has a broad pattern of expression in both male and female reproductive tissues, including epididymosomes and uterosomes (uterine S-EVs)[83,114]. SPAM1 acts as a hyaluronidase in penetrating the cumulus complex, and as a secondary sperm–ZP binding protein in acrosome-reacted sperm[201,202], and is particularly active under neutral-pH conditions, such as those within the uterus and fallopian tubes during ovulation[203] (Fig. 3). Epididymal SPAM1 has been shown to be transferred by epididymosomes to sperm, probably during sperm maturation in the epididymis[83]. *Spam1*-knockout mice sperm can penetrate the cumulus and fertilize the oocyte, the COC entry and cumulus navigation is impaired[204]. Thus, reduced content of SPAM1 might serve as a marker of poor cumulus entry and penetration, highlighting a major component of both natural conception and conventional IVF (Table 1).

Parkinson disease protein 7. Parkinson disease protein 7 (PARK7) is a multifunctional protein with possible involvement in protection from oxidative stress[205], neuroprotection[206] and male fertility[207] and has been identified in epididymosomes surgically retrieved from vasectomized men[63]. Immunocytochemical analysis has identified PARK7 all throughout the male reproductive system including Leydig and Sertoli cells and sperm flagellar, suggesting functions in spermatogenesis and sperm motility, respectively[208,209] (Fig. 3). PARK7 down-regulation has been observed in men with asthenozoospermia and has been attributed to poor oxidative stress management, causing reduced sperm motility[207,210]. A positive correlation was found between PARK7 expression and sperm superoxide dismutase (SOD) activity, leading to the hypothesis that PARK7 modulates SOD activity and has been supported by *PARK7*-knockdown cells showing reduced *SOD3* expression[207,211] (Table 1). Reduced PARK7 expression might serve as a biomarker of increased exposure of sperm to oxidative stress during epididymal transit.

Seminal plasma S-EV microRNAs

S-EV miRNAs negatively modulate diverse biological functions at the post-translational level by inhibiting specific mRNA targets within target cells by binding to the 3′-untranslated region (UTR) of their target mRNAs and inhibiting protein synthesis by destabilizing the mRNA and translational silencing[14,212–214]. The miRNA contents of seminal plasma S-EVs differ greatly: substantially variable miRNA content was detected in epididymosomes from each portion of the epididymis[64]. Furthermore, studies have shown considerable biological value to measurable miRNA content in both prostasomes[142,215,216] and epididymosomes[217–219].

miRNA content patterns in seminal plasma S-EVs have the potential, along with proteins, to serve as biomarkers for pathophysiological states and have already been proposed as markers of prostate cancer[216] and azoospermia[220]. Encapsulation of miRNAs within S-EVs provides protection from extracellular conditions and enzymes while providing a more accurate representation of intercellular communication than circulating free miRNA that is possibly released by apoptotic bodies and cellular debris[37]. In one study, miRNA markers within seminal plasma S-EVs that could enable non-invasive prediction of whether surgical sperm collection was viable in men with azoospermia were identified[205]. First, miR-31-5p content in S-EVs in combination with blood follicle-stimulating hormone (FSH) concentration was proposed to identify samples from men with obstructive conserved spermatogenesis or spermatogenic failure. Second, levels of miR-539-5p and miR-941 can be used as a method of identifying residual sperm in the testes. The results of this study corroborate associations between aberrant cell-free miRNA levels in semen and deviations in sperm quality in both whole seminal plasma[221,222] and in S-EVs[223]. Comparison of seminal plasma S-EV miRNA from men with oligoasthenozoospermia with men with normozoospermia showed increased levels of miR-765 and miR-1275 and a reduced level of miR-15a[208]. Furthermore, variable content of different RNAs in seminal plasma S-EVs from samples resulting in intrauterine insemination pregnancies versus failures has been observed, although this observation was not specific to miRNAs[209].

As with proteomic analysis of S-EV contents, miRNA biomarker discovery relies on highly purified populations of S-EVs; therefore, contaminants can distort observations and conclusions made during deep sequencing of nucleic acids. Thus, optimizing S-EV purification, performing diverse and comprehensive miRNA discovery analysis and ultimately consolidating a biomarker panel, has the potential for personalized, point-of-need diagnostics in ART.

Clinical utility of seminal plasma S-EVs

The current diagnostic approaches to identifying causes of idiopathic and male-factor infertility begin with general health assessments, as well as clinical assessment of semen parameters such as those described by the WHO[224]. Semen diagnostics currently focus on observable semen characteristics and sperm functional parameters including semen volume, sperm concentration, motility, viability and morphology[224]. Sperm DNA fragmentation can also be assessed, indicating oxidative stress-based damage caused to sperm within the male reproductive system that has substantial negative effects on fertility[225]. Additionally, congenital genetic abnormalities identified using chromosomal analysis contribute to 15–20% of severe instances of male-factor infertility, whereas ~60% are idiopathic[226]. Other commonly identified causes of male-factor infertility are reproductive system anatomical

complications (including epididymitis and varicocele), testicular failure, anti-sperm antibodies and epigenetic changes[227]. The inability of health assessment and semen parameters to elucidate causes of idiopathic infertility, owing to considerable overlap of these parameters between fertile and infertile men, highlights the need for actionable molecular approaches to semen diagnostics.

The protein and miRNA landscape of seminal plasma S-EVs has been identified as a method of indicating sperm dysfunction with the accumulation of the knowledge of protein and miRNA origin and biological function, as well as differential content of these protein and miRNAs within S-EVs from fertile and infertile men[108,149,159,228]. Using S-EVs for infertility diagnostics in ART requires three key components for routine adoption: first, an effective, simple and fast method of S-EV isolation from semen or seminal plasma, which would require a highly purified population of S-EVs, devoid of contaminants, whereby targeted analysis could identify sub-populations of S-EVs and/or measure relative abundance of specific proteins and nucleic acids, with pre-determined normalization and reference values; second, a robust panel of biomarkers that have been shown in randomized-controlled trials to have statistically significant correlations with specific deficiencies in sperm functions (such as sperm maturation, capacitation, acrosome reaction, motility, DNA fragmentation, sperm–ZP binding and sperm–oolemma membrane fusion) and subsequent downstream effects after oocyte fertilization; and third, an actionable output of information with statistical power, informing clinicians and scientists on how to personalize the treatment of a patient having undergone such a test. For example, biomarkers indicating dysfunction in sperm capacitation or interaction with the cumulus-oocyte-complex would indicate ICSI over conventional IVF, whereas those indicating poor blastocyst development might suggest earlier cleavage-stage embryo transfer rather than day 5 or 6 embryo transfer. Biomarkers of repetitive implantation failure or miscarriage might indicate pre-implantation genetic testing for aneuploidy to select euploid embryos. Using these tools could create a molecular method of reducing repetitive cycles for patients undergoing infertility treatment, whereby unsuccessful cycles are inadvertently used as pseudo-diagnostics to manipulate subsequent treatment approaches yet come with a substantial financial, emotional and physical cost for patients.

Isolation of S-EVs

Considering the considerable advances in separation science and cell isolation technology, isolating S-EVs as a pure population remains extremely difficult, particularly the differentiation of various subtypes of S-EVs and EVs of similar size from a highly heterogenous biofluid such as blood. To date, no fast, inexpensive, portable method of isolating S-EVs from seminal plasma or whole semen exists. Seminal plasma S-EVs have been studied by implementing and adapting conventional methods optimized for other body fluids as their clinical and diagnostic value increased[55,142,229]; however, difficulties arise when the processes involved rely on multiple, laborious ultracentrifugation steps at various temperatures and require high initial volumes of sample to isolate a relatively pure population of S-EVs. Contamination by non-S-EV proteins and extracellular subpopulations is common, which inevitably causes incorrect or inaccurate deductions from quantitative biomarker analyses and other specific conclusions made from these samples[230]. These traditional and sometimes out-dated methods have also been observed to interfere with the structural morphology of native S-EVs[231,232], distorting the reality of how these vesicles are structured and the mode by which they function. Additionally, the lack of portability and access to isolation methods in clinical settings can cause contamination and increased background when biofluids are cryopreserved before processing, whereby disruption of vesicles and cells causes protein and nucleic acid leakage, preventing pure samples of S-EVs from being isolated downstream[233]. With high-resolution next-generation sequencing for quick profiling of miRNA and liquid chromatography–tandem mass spectrometry for complex protein analysis, innovative and accurate methods of S-EV isolation have the potential to open up avenues of personalized medicine that have been previously neglected in ART.

The S-EV isolation approach must be tailored according to needs and outcome of analyses. For example, diagnostic research and studying S-EV protein content can be approached in a global, exploratory mode or a targeted biomarker analysis. These metrics can be highly influenced by contamination, poor technique and operator variability, therefore, careful selection of a method is required. Isolation of S-EVs for therapeutic purposes is a field in which S-EVs are used as possible target delivery mechanisms for drugs and biomolecules to treat disease and/or altered physiological states[234,235]. The International Society for Extracellular Vesicles (ISEV) recommends specific conventional approaches to experimental requirements based on S-EV specificity and recovery capabilities, as well as initial biofluid complexity[236]. Conventional approaches to S-EV isolation thereby fall into four categories according to the ISEV recommendations: high recovery with low specificity; intermediate recovery with intermediate specificity; low recovery with high specificity; and high recovery with high specificity. However, high recovery with high specificity is considered by the ISEV to be unachievable with current technology[236]. These recommendations remain broad and require thorough interpretation by researchers and operators and a clear understanding of experimental or clinical requirements and outcomes.

Conventional methods of isolating EVs include precipitation, differential and gradient density ultracentrifugation, size-exclusion chromatography (SEC), immune-affinity-based isolation and ultrafiltration[218]. The rapidly evolving field of microfluidics and integration with immunoaffinity-based capture, membrane-based filtration, nanowire trapping, acoustic nanofiltration, deterministic lateral displacement (DLD) and viscoelastic flow sorting, is enabling this technology to be used as a possible method of S-EV isolation for liquid biopsies[218].

Conventional methods of S-EV isolation

Conventional methods of S-EV isolation are widely used and have largely been developed and optimized for blood and conditioned media and rarely for semen and seminal plasma. Raw semen and seminal plasma present similar challenges to blood, yet require adaptations to overcome the specificities of the fluid. As with blood, semen has both a cellular fraction (sperm, immature germ cells, leukocytes and epithelial cells) and an acellular fraction (seminal plasma)[237]. However, isolation of S-EVs from raw semen presents a unique challenge in that sperm are motile and highly heterogenous from different donors or between ejaculates of the same donor. Simple, low-speed centrifugation is effective at isolating sperm from semen, resulting in seminal plasma. Approaches to isolating S-EVs from semen are relatively uniform, in that most of these techniques begin with a simple, low-speed centrifugation step to remove large cells and particles, then either polymer precipitation or ultracentrifugation combined with SEC, gradients or filtration (Table 2).

Precipitation. Precipitation of S-EVs from biofluids has become a highly commercialized method of S-EV isolation as the need for ultracentrifugation is removed, improving accessibility and ease[238].

Table 2 | Studies on seminal plasma S-EV isolation

Field of study	Centrifugation	Ultracentrifugation	SEC	Gradient	Filtration	Precipitation	Specifics	Organism	Ref.
HIV	✓	✓	X	X	X	✓	ExoQuick precipitation	Human	229
HIV	✓	✓	X	X	X	✓	ExoQuick precipitation	Human	243
HIV	✓	✓	X	X	X	✓	ExoQuick precipitation	Human	246
HIV	✓	✓	X	X	X	✓	ExoQuick precipitation	Human	345
HIV	✓	✓	X	X	X	✓	ExoQuick precipitation	Human	244
HIV	✓	✓	X	X	X	✓	ExoQuick precipitation	Human	245
Prostasome analysis	✓	X	✓	X	X	X	NA	Human	143
Prostasomes improving swim-up sperm isolation efficiency	✓	✓	✓	X	X	X	NA	Human	346
Prostasome analysis	✓	✓	✓	X	X	X	NA	Horse	347
Prostate cancer prostasomes	✓	✓	✓	X	X	X	NA	Human	348
Prostasome analysis	✓	✓	✓	X	X	X	NA	Human	61
Epididymosome and prostasome analysis in patients undergoing vasectomy reversal	✓	✓	✓	X	X	X	Epididymosomes: differential centrifugation; Prostasomes: differential centrifugation and SEC	Human	63
Prostasome function	✓	✓	X	✓	X	X	Sucrose gradient	Human	55
Prostate cancer prostasomes	✓	✓	✓	X	X	X	NA	Human	349
Prostasome function	✓	✓	✓	X	X	X	NA	Human	139
Progesterone-induced sperm motility	✓	✓	✓	X	X	X	NA	Human	27
Association of cystatin C with prostasomes in human seminal plasma	✓	✓	✓	X	X	X	NA	Human	350
Prostasome analysis	✓	✓	✓	✓	X	X	Sucrose block gradient	Human	134
Sperm capacitation	✓	✓	✓	✓	X	X	Sucrose block gradient	Horse	28
S-EV function (RNA)	✓	✓	X	✓	X	X	Sucrose cushion gradient	Human	142
S-EV miRNAs	✓	✓	X	✓	X	X	Sucrose cushion gradient	Human	351
Sperm function	✓	✓	X	X	✓	X	Nanofiltration	Pig	352
Prostasome analysis from normospermic versus non-normospermic men	✓	✓	X	X	X	X	NA	Human	159
Azoospermia	✓	✓	X	X	✓	X	Microfiltration	Human	220
Prostate cancer	✓	✓	X	X	✓	X	Microfiltration	Human	216
Sperm motility and S-EVs	✓	✓	X	X	X	X	NA	Human	25
Oligozoospermia	✓	✓	✓	X	X	X	NA	Human	353
Epididymosome role in sperm maturation	✓	✓	X	✓	X	X	Discontinuous iodixanol gradient ultracentrifugation	Mice	97

miRNA, microRNA; NA, not applicable; SEC, size-exclusion chromatography; S-EV, small extracellular vesicle.

Currently, two common approaches to S-EV precipitation exist, both of which require conventional centrifugation at lower speeds than ultracentrifugation (<10,000 g): polymer precipitation, which induces S-EV precipitation based on binding of hydrophilic polymers to water molecules surrounding S-EVs (Fig. 4Aa); and two-phase precipitation, which consists of a hydrophilic and hydrophobic solution added to a biofluid, enabling accumulation of S-EVs and other EVs in the hydrophilic phase after centrifugation (Fig. 4Ab). Both methods of precipitation produce higher S-EV purity and recovery than ultracentrifugation, assessed via size-distribution and concentration within the output solution[239–241], yet risk damaging S-EVs and the precipitation matrices might influence S-EV biological activity and cargo characteristics[238,242].

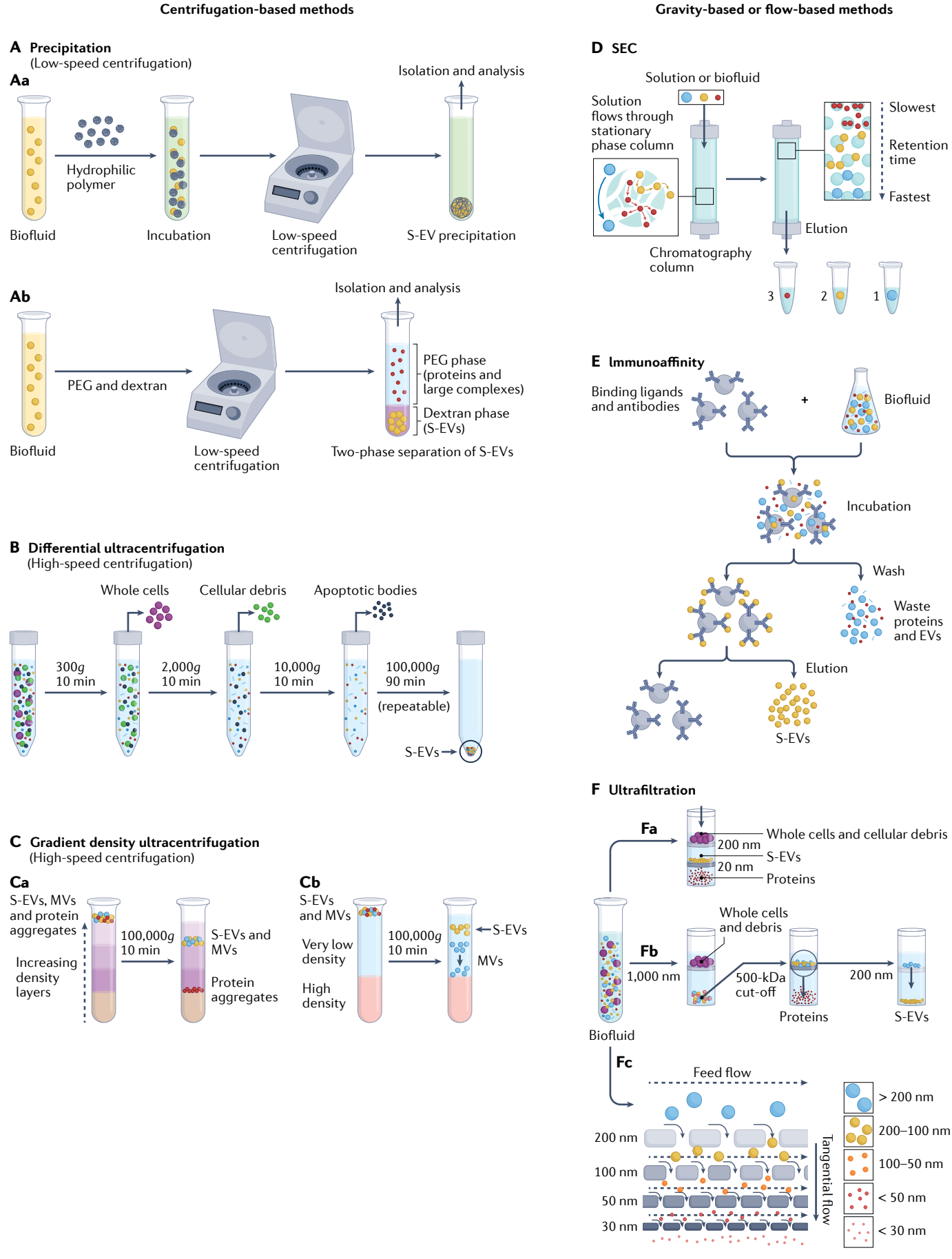
Centrifugation-based methods
Gravity-based or flow-based methods
A Precipitation
(Low-speed centrifugation)
Aa
Isolation and analysis
Hydrophilic polymer
Biofluid
Incubation
Low-speed centrifugation
S-EV precipitation
Ab
Isolation and analysis
PEG and dextran
PEG phase (proteins and large complexes)
Dextran phase (S-EVs)
Biofluid
Low-speed centrifugation
Two-phase separation of S-EVs
B Differential ultracentrifugation
(High-speed centrifugation)
Whole cells
Cellular debris
Apoptotic bodies
300g 10 min
2,000g 10 min
10,000g 10 min
100,000g 90 min
(repeatable)
S-EVs
C Gradient density ultracentrifugation
(High-speed centrifugation)
Ca
S-EVs, MVs and protein aggregates
Increasing density layers
100,000g 10 min
S-EVs and MVs
Protein aggregates
Cb
S-EVs and MVs
Very low density
High density
100,000g 10 min
S-EVs
MVs
D SEC
Solution or biofluid
Solution flows through stationary phase column
Chromatography column
Slowest
Retention time
Fastest
Elution
3
2
1
E Immunoaffinity
Binding ligands and antibodies
+
Biofluid
Incubation
Wash
Waste proteins and EVs
Elution
S-EVs
F Ultrafiltration
Fa
200 nm
20 nm
Whole cells and cellular debris
S-EVs
Proteins
Fb
1,000 nm
Whole cells and debris
500-kDa cut-off
Proteins
200 nm
S-EVs
Biofluid
Fc
Feed flow
200 nm
100 nm
50 nm
30 nm
Tangential flow
> 200 nm
200–100 nm
100–50 nm
< 50 nm
< 30 nm

Fig. 4 | Conventional methods of isolating S-EVs and EVs from biofluids. **A**, Precipitation: polymer precipitation (part **Aa**) and two-phase precipitation (part **Ab**). **B**, Differential ultracentrifugation. **C**, Gradient density ultracentrifugation: isopycnic density-gradient ultracentrifugation (part **Ca**) and the moving-zone gradient ultracentrifugation (part **Cb**). **D**, Size-exclusion chromatography (SEC). **E**, Immunoaffinity-based small extracellular vesicle (S-EV) isolation. **F**, Ultrafiltration: tandem-configured microfiltration (part **Fa**), sequential ultrafiltration (part **Fb**) and tangential flow filtration (part **Fc**). EV, extracellular vesicle; MV, microvesicle; PEG, polyethylene glycol; S-EV, small extracellular vesicle. Adapted from ref.[260], CC BY 4.0 (https://creativecommons.org/licenses/by/4.0/).

Polymer-based methods commonly involve the use of polyethylene glycol (PEG), which has been adopted and used to effectively isolate highly purified S-EVs from large volumes of biofluids using a method called ExtraPEG, which involves overnight PEG incubation at 4 °C, but requires a short ultracentrifugation step[225]. Furthermore, a technique to coat Fe_3O_4 magnetic nanoparticles with PEG has been developed to remove contaminating protein aggregates from serum S-EV isolates, improving S-EV purity when performing highly sensitive protein analysis[226]. Commercial kits for S-EV isolation based on polymer precipitation are available, such as the ExoQuick portfolio (System Biosciences), which has been shown to be highly effective for isolating and purifying S-EVs from semen[243–246], serum[247,248], human breast milk[249] and bovine milk[250] (Table 2). Commercial precipitation-based kits require lower sample input volumes (<1 ml) than ultracentrifugation (>1 ml)[241] and are relatively simple to operate, but they have limited specificity for various S-EV populations, are relatively high cost and require further processing to remove precipitants before being analysed[251].

Ultracentrifugation. Ultracentrifugation is the gold-standard particle separation technique based on size, consisting of sequential centrifugation of the sample at progressively increasing speeds[252]. Cells, apoptotic bodies and large EVs are separated by initial centrifugation steps below 20,000*g* and S-EVs are isolated from protein aggregates using subsequent ultracentrifugation above 100,000*g* (Fig. 4B). This process requires high sample volume (millilitres) input owing to low recovery yield (5–25%) and long processing times[253]. Additionally, contamination with particles of similar size as well as particulates and protein aggregates cause decreased purity[254,255]. Furthermore, specialized equipment is required for ultracentrifugation, which might not be accessible to routine clinic and hospital laboratories and requires training and a dedicated team owing to long run times (>4 h)[256,257]. This low recovery yield has been improved with incorporation of gradient density-based ultracentrifugation, such as isopycnic density-gradient ultracentrifugation (particle density-based separation) (Fig. 4Ca) and moving-zone gradient ultracentrifugation (particle density and mass–size separation)[258,259] (Fig. 4Cb). Many seminal plasma S-EV isolation methods make use of ultracentrifugation (Table 2), most probably owing to the extremely high concentration of S-EVs in seminal plasma, negating the need for high recovery yields if labour, time and equipment are available[25].

Size-exclusion chromatography. SEC has been used to remove S-EVs from fluids containing contaminants and protein aggregates in which pre-centrifugation is often required to remove large cells, EVs and cellular debris[260]. The sample solution then flows through a stationary phase column containing a porous matrix using gravity, trapping and slowing of the flow of small particles and permitting faster elution of large particles (Fig. 4D). Thus, particles can be isolated based on size according to the time taken to flow through the stationary column. S-EV purity (based on size determination and albumin contamination) and structural integrity (determined via electron microscopy) are high with SEC; however, run times (owing to gravity often being the flowing force), yield and input volumes require improvement compared with other techniques[261,262]. Combinations of ultracentrifugation and SEC are often used to isolate S-EVs from seminal plasma with fairly good results (Table 2), but a series of laborious processing steps remain to reach unspecific populations of S-EVs. Commercial systems, such as the qEV Isolation platform (IZON Science), integrate a proprietary SEC column with an automatic fraction collector, which automates collection of eluents, minimizing labour requirements and improving the purity of size-based EV isolation, but are a relatively expensive investment[263–265]. Exo-spin™ (Cell Guidance Systems) provides a modular system, adaptable to various requirements, enabling users to customize their column based on biofluid input, and to be effective at purifying S-EV populations from cancer cell lines[266], serum[267] and plasma[240].

Immunoaffinity-based isolation. S-EVs have unique surface markers[268]; therefore, specific antibody binding affords the option to target populations of S-EVs and EVs in a heterogenous solution. S-EVs have ubiquitous surface protein markers regardless of origin, as well as organ-specific or tissue-specific markers, which give immunoaffinity-based methods increased specificity when it comes to studying S-EVs[269]. Antibodies can either be immobilized on a stationary surface or on particles such as magnetic beads, which bind to specific S-EV populations in a biofluid, enabling simple elution of S-EVs with subsequent steps (Fig. 4E). S-EV purity and specificity remain high owing to S-EV-specific antibodies selected (such as EpCAM or CD63), depending on unintended binding of antibodies to collateral cells and vesicles, sample volume processing capacity is limited[257,270]. Purity is assessed via immunostaining, western blotting and size-determination methods. S-EV recovery yields are lower than other methods and reagents are often costly, yet separation time is low and biofluid pre-processing is not required[271]. Comparison of immunological separation techniques with ultracentrifugation showed drastic improvements in yield (at least two-fold more) and purity of S-EVs based on quantification of common S-EV protein markers such as ALIX, TSG101, CD9 and CD81 (refs.[252,253]). Several immunoaffinity-based kits are commercially available for S-EV isolation, such as the MACSPlex Exosome Kit (Miltenyi Biotec), consisting of a multiplex approach, and enable up to 37 surface epitopes for continuous flow cytometric detection of S-EVs within a biofluid. This kit provides a broad spectrum of detection for comprehensive and customizable detection of S-EVs for variable approaches.

Ultrafiltration. Filtration-based approaches to S-EV isolation are simple but often require integration with ultracentrifugation to separate S-EVs from protein aggregates of S-EV-sized nanoparticles after filtration[240]. Membranes with nanopores for size-based isolation of particles from a fluid can be used in various configurations[260]. Tandem-configured microfiltration consists of two or more nanofilters of known exclusion sizes, arranged in a vessel that allows particles of desired size to flow through (Fig. 4Fa). Sequential ultrafiltration requires multiple steps of filtration through different vessels based on size (Fig. 4Fb). Tangential flow filtration (TFF) isolates particles from a sample feed stream, flowing parallel to a sequence of membranes of decreasing pore size, with a perpendicular tangential flow pressure directing particles through the membranes (Fig. 4Fc). Filtration is considerably faster than ultracentrifugation but often requires high sample input volumes with substantial risk of low S-EV recovery, owing to pore clogging[257,272]. A major problem with filtration-based methods is membrane surface binding by vesicles and S-EVs that clog the membrane pores and drastically reduce sample purity[273]. Membrane pore clogging can theoretically be avoided with repetitive washing steps;

however, this process adds substantial amounts of processing time to each step. Ultrafiltration relies solely on size selection; therefore, S-EV purity is high based on size distribution; however, proteins and other nanoparticles are also selected[273]. Thus, extra selection for S-EV subpopulations and removal of protein and debris contaminants are required. A benefit of ultrafiltration is that large, specialized equipment is not required and many techniques only require simple, low-speed centrifuges. Commercial products such the EV spinner and TFF filters from HansaBioMed Life Sciences, are effective S-EV purifiers for use in conjunction with centrifugation[274]. Ultrafiltration has large scalability potential but with increasing flow pressures, shear stress and clogging might cause EV membrane damage and reduced EV output; however, automated TFF arrays running at low pressures with programmed washing and elution steps could negate these issues[275,276].

The effectiveness of conventional methods of S-EV isolation relies heavily on the heterogeneity and complexity of biological samples and they often provide results that are dependent on substantial pre-processing and debulking of collateral cells and contaminants before separation. The biochemical and physiological properties of EVs and S-EVs make the output of these techniques highly variable and operator dependent, without combining multiple techniques for improved results. For example, combining ultracentrifugation with targeted immunoaffinity capture can isolate S-EVs from the S-EV, protein and lipoprotein pellet created from only performing ultracentrifugation. However, these processes are associated with considerable time and costs and require complex equipment and dedicated staff to operate it. Microfluidics can integrate these methods and other methods enabled only by the geometry and physics of microfluidic platforms, in a simplified, cost-effective and user-friendly format, therefore enabling routine use of S-EVs in medicine.

Microfluidic S-EV isolation and detection

Microfluidics is the study and manipulation of small volumes of fluid at the micrometre scale[29], and in the context of S-EV isolation, relies upon the physical and biochemical properties of S-EVs including size, density, charge and surface proteins present to perform isolation[256].

In 1990, Manz et al.[277] pioneered microfluidic particle separation by showing the efficiency of electrophoretic separation in a "micro total analysis system" (μ-TAS), when compared with conventional electrophoresis; consequently, the use of microsystems capable of incorporating sampling, sample pre-treatment, separation and detection was proposed. Microfluidics has since evolved into a robust approach to miniaturizing, often simplifying conventional laboratory equipment[251,278,279] and has shown promise for applications in infertility treatment with sperm selection from motile[280–282] and azoospermic surgical samples[283–285], as well as routine use in clinical embryo and oocyte cryopreservation[286]. Commercial success has been achieved using microfluidic products both in sperm selection (such as the ZyMōt catalogue (ZyMōt Fertility)) and in embryo and oocyte cryopreservation (such as the Gavi® automated vitrification system (Genea Biomedx)). Microfluidic sperm selection is based on fundamentally different science from the isolation of S-EVs dictated primarily by size differences in target cells or molecules. Sperm are motile and are ~55 000 nm in length, whereas the diameter of an S-EV is 30–150 nm (refs.[13,287]). Thus, the physics and geometry of sperm isolation microfluidic platforms are much larger and can work using static fluidics to exploit sperm motility or considerable differences in cell sizes[283], whereas S-EV isolation requires flow and specific chemistry and physics to target S-EVs from other particles[253].

Conventional isolation methods are often combined to create optimized protocols with increased S-EV yield and purity, but the inherent weaknesses of each method can persist and are not fully overcome. However, microfluidics can combine conventional approaches on a single miniaturized platform, typically requiring drastically reduced sample input volumes and exploiting S-EV-specific physiology, chemistry and physics. Thus, microfluidics can enable isolation, detection, characterization and analysis of S-EVs from biofluids on a single platform. Isolation of S-EVs using microfluidics has been performed using multiple approaches, based on conventional methods such as immunoaffinity-based isolation and filtration, as well as novel techniques such as deterministic lateral displacement (DLD), acoustic nanofiltration and nanowire trapping (Table 3).

Most microfluidic S-EV isolation platforms are purpose-built for cancer diagnostics with a blood-based or urine-based liquid biopsy approach. No semen or seminal plasma S-EV diagnostic devices exist, possibly because of the lack of consensus on S-EV importance in reproduction or the value of S-EV diagnostics in fertility. Furthermore, many of these devices have been designed to provide a point-of-care model to cancer diagnostics, whereas, if applied to infertility diagnostics, a point-of-need model would be more practical. Point-of-need diagnostics will help to shape and direct treatment before or during ART procedures. For general diagnostics, input volumes of liquid biopsies are often kept low but not at the expense of providing clinical significance. Biofluids, particularly semen, are highly heterogenous in nature but have an extremely high concentration of S-EVs[55]. Available volumes vary greatly between patients and often limit functionality if recovery yields are low, providing clinically insignificant amounts of S-EVs for analysis when processed with conventional methods. In this regard, the microfluidic isolation of S-EVs benefits from the innate ability to process small volumes of biofluids and when using microfluidic platforms for on-chip detection of specific S-EV populations or surface markers: limit of detection (LOD) is an important performance metric and depends largely on the target S-EV concentration within a given biofluid[288]. For example, healthy semen has trillions of S-EVs per ejaculate, reducing the importance of LOD. However, in the case of therapeutics, the scalable processing of biofluid volumes for bulk preparation of S-EVs is difficult and limits their commercial viability.

S-EVs are identified and counted using physical analysis methods, such as NTA, dynamic light scattering as well as scanning electron microscopy and transmission electron microscopy. These methods are effective at measuring S-EV size, concentration, and homogeneity, and are often used to validate these methods. However, an important caveat is the developer bias with idealizing representations of device performance based on simple, processed samples, such as conditioned media or highly processed and isolated S-EV samples, which might not equate to biofluids with increased complexity, such as whole blood. For example, recovery yield reporting might be misleading and should be analysed critically when deciding which technique suits specific requirements. S-EV capture efficiency is often quantified using relative protein content (Table 3), which has obvious flaws when considering soluble protein contaminants in complex biofluids. More complex investigation of S-EVs and their contents is performed using biochemical and compositional analysis based on immunodetection, flow cytometry, western blotting, enzyme-linked immunosorbent assays (ELISA), mass spectrometry and PCR-based analysis of nucleic acids.

Detection and quantification of specific S-EVs post-isolation is commonly performed using flow cytometry; therefore, simplifying and improving flow cytometry workflows and equipment have garnered

Table 3 | Microfluidic approaches to S-EV isolation and detection[a]

Method and description	Field of application	Sample	Input volume (µl)	Flow rate (µl/min)	Recovery yield (%)	Isolation size (nm)	Ref.
Acoustic isolation							
Continuous acoustic nano-filtration	Ovarian carcinoma diagnostics	Ovarian carcinoma cells (OvCA429) (ultracentrifuged)	50	~0.24	>80	~30–200	354
Dual-module, cell-removal and S-EV isolation, acoustic filtration device using tilted angle standing sequential surface acoustic wave	General blood diagnostics	Whole blood	100	4	82	<150	312
Acoustic trapping of S-EVs within seed particles using scattered sound particle aggregation on an 'AcouTrap' instrument	General biomarker diagnostics	Conditioned culture media, urine and plasma samples (ultracentrifuged)	300–5,000	15	NA	30–500	355
Acoustofluidic S-EV and lipoprotein isolation using standing surface acoustic waves	General blood diagnostics	Plasma	Continuous flow with pump	0.5 (dual inlets)	NA	20–600	356
Dielectrophoretic separation							
ACE microarray chip with dielectrophoretic separation force	Glioblastoma diagnostics	Plasma or buffer spiked with glioblastoma S-EVs and EVs	30–50	~3–5	NA	50–150	317
iDEP chip with borosilicate micropipette microarrays	General biomarker diagnostics	Healthy serum, saliva and conditioned media	200	NA	NA	30–150	357
Microsphere-mediated immunocapture and detection with DEP integration on 'ExoDEP-chip'	Cancer diagnostics	Conditioned media from adenocarcinomic alveolar basal epithelial cells (A549), HEK293 cells and hepato-cellular cancer cells (HepG2) (ultracentrifuged and diluted)	Continuous flow with pump	1	83.5	<150	318
DLD							
DLD-based size exclusion array	Pancreatic cancer diagnostics	BxPC-3 (pancreatic epithelial cells), extracellular shed vesicles (centrifuged) and packed RBC units	3,500	NA	39	<250	320
Nano-DLD sorting using micropillar array	General blood diagnostics	Commercial urine-derived S-EVs	Continuous flow with pump	0.003	NA	20–110	358
Nano-DLD sorting using micropillar array	Prostate cancer diagnostics	Serum and urine from patients with prostate cancer	1,000	15	50	30–200	35
FlFFF							
FlFFF microfluidic separation based on hydrodynamic diameter	General biomarker diagnostics	HB1.F3 immortalized human neural stem cell isolated S-EVs in solution (centrifuged)	Continuous flow with pump	45	NA	30–120	325
Immunoaffinity (targeted marker)							
Functionalized (CD63) channel with herringbone grooves	Cancer diagnostics	Serum (filtered)	400	13.1	42–94	20–135	293
Modified mica disc surfaces (CD41) with flow cell	General blood diagnostics	Plasma (centrifuged and diluted)	10	10	NA	30–140	295
Functionalized (CD63) multi-chamber and channel device 'ExoChip'	Pancreatic cancer diagnostics	Pancreatic cancer patient and healthy serum	400	4	NA	~30–300	34
Reusable 'nPLEx' assay: functionalized flow cell (CD24, CD63 and EpCAM) with gold-layered nanoholes and gold nanoparticle secondary labelling	Ovarian cancer diagnostics	Ascite samples from ovarian cancer cells (filtered)	Continuous flow with pump	10	NA	~100	298
Immunomagnetic (EpCAM, IGF1R, CA125, CD9, CD63 and CD81) microbeads	Lung cancer diagnostics	Plasma from patients with lung cancer (pre-mixed with microbeads)	30	2	NA	~40–250	232
Capture on functionalized (CD9 and HER2) gold electrodes using alternating current-induced nanoshearing	Breast and prostate cancer diagnostics	Serum from patients with breast cancer and breast cancer (BT-474 and MDA-MB-23) and prostate cancer (PC3) cell line S-EVs (centrifuged) in PBS.	500	4.2	NA	~30–350	299

Table 3 (continued) | Microfluidic approaches to S-EV isolation and detection[a]

Method and description	Field of application	Sample	Input volume (µl)	Flow rate (µl/min)	Recovery yield (%)	Isolation size (nm)	Ref.
Immunoaffinity (targeted marker) (continued)							
Immuno-magnetic S-EV RNA 'iMER' analysis using immunomagnetic beads (EGFR) and RNA isolation and real-time PCR integration	Glioblastoma cancer diagnostics	Serum from patients with glioblastoma (filtered) and GBM cell lines	100	4	93	<100	297
Continuous immunomagnetic (CA125, EpCAM and CD24) microbead capture 'ExoSearch'	Ovarian cancer diagnostics	Plasma	20	0.8	72	~50–250	300
Immunocapture (CD63, CD81 and EpCAM) on graphene oxide and polydopamine-coated, Y-shaped microposts with the 'nano-IMEX' platform	Ovarian cancer diagnostics	Plasma (diluted)	20	0.05	NA	<150	296
Two-step sandwich approach with functionalized (CD9 and CD63) gold surface and cancer-specific S-EV capture (HER2)	Breast cancer diagnostics	BT474 breast cancer cell-line and breast cancer patient serum	250	5	NA	~30–300	301
Smartphone-enabled optofluidic platform using negative (CD45 and CD61) and positive (CD81) enrichment with microbeads of different size 'µMED'	Brain trauma diagnostics	Rat neuronal cell S-EVs and mouse serum	~100	<10	NA	~117	302
Capture on immunomagnetic (CD63) particles	Breast cancer diagnostics	Plasma from healthy individuals and patients with breast cancer (pre-incubation with capture particles) and breast cancer cell lines	~1,000	2	NA	<100	294
'ExoPCD-chip' with magnetic bead (TIM4) to isolate CD63-positive S-EVs, with Y-shaped micropillars and electrochemical sensor	Liver cancer diagnostics	HepG2 cell line (centrifuged) and serum from patients with liver cancer	30	0.2	68.5	<150	32
Functionalized (CD63 and EpCAM) channels with herringbone pattern	Ovarian cancer diagnostics	Serum from patients with HGSOC (filtered)	100	20	~60	30–150	303
Functionalized (CD63 and EpCAM) channels with herringbone pattern	Ovarian cancer diagnostics	Serum from patients with HGSOC (filtered), HGSOC cell lines, ovarian surface epithelial cells and fallopian tube secretory epithelial cells	100	20	NA	NA	291
Functionalized (CD81, EpCAM, FRα) 3D-herringbone nanostructure immunocapture in 'Nano-HB chip'	Ovarian cancer diagnostics	Plasma	20–100	0.5	76.5–80	40–160	33
Micropillar-based PDMS chip (CD9) queuing functionalized beads and quantum dot probes	Lung cancer diagnostics	Plasma from patients with lung cancer (centrifuged)	80	3	NA	~25–250	359
Dual-module isolation of CTCs and S-EVs using immunocapture (MCAM and MCSP) on 'dual-utilization OncoBEAN' (DUO)	Melanoma diagnostics	Plasma from patients with melanoma (filtered)	1,000	16.7	75	'S-EV size'	304
Simple continuous flow microfluidic device using magnetic bead capture (CD9)	Pancreatic cancer diagnostics	Whole blood from patients with pancreatic cancer	Continuous flow with pump	50	NA	130	292
Magnetic bead immunocapture (CD63) on triangular pillar array and integrated Raman detection region with EpCAM-functionalized Raman beads	Prostate cancer diagnostics	Serum from patients with prostate cancer and healthy donors	20	0.6	72.5	100	36
Membrane-based filtration							
Pressure-based filtration	Melanoma diagnostics	Mouse whole blood	3	0.075	>1.5	~150	360
Electrophoresis-based filtration	Melanoma diagnostics	Mouse whole blood	240	2	1.5	~150	360
Electrophoretic filtration on nanoporous membrane	General diagnostics	Mouse plasma (diluted)	1000	20	65	10–400	361
Dual-filtre centrifugal microfluidic 'Exodisc'	Cancer diagnostics	Urine	1,000	36	>95	20–600	323

Table 3 (continued) | Microfluidic approaches to S-EV isolation and detection[a]

Method and description	Field of application	Sample	Input volume (µl)	Flow rate (µl/min)	Recovery yield (%)	Isolation size (nm)	Ref.
Membrane-based filtration (continued)							
Dual-filtre channel with on-chip ELISA-based (CD63) detection	Bladder cancer diagnostics	Urine (centrifuged and filtered)	8,000	33	74.2	155	362
Modular 'ExoTIC' multi-membrane sequential filtre units	Lung cancer diagnostics	Blood plasma, urine, and lung BAL fluid from patients with non-small-cell lung cancer (diluted)	500	25	NA	30–200	309
Dual-module filtration and immunocapture	Biomarker diagnostics	Whole blood and PFP	500	22	94	50–200	278
Double nanofiltre 'ExoID-Chip' with integrated photonic crystal nanostructure	Breast cancer diagnostics	Serum from patients with breast cancer (centrifuged)	20	10	NA	20–200	363
Electrophoretic filtration on nanomembrane 'ExoSMP'	Cancer diagnostics	MDA-MB231 cancer cell line-derived small EVs (ultracentrifuged)	500	5, 10 and 20	94.2	30–120	310
Pressure-based filtration and CD63 antibody immunoaffinity-based capture	Liposarcoma diagnostics	LPS cell lines (centrifuged) and serum from patients with LPS (centrifuged)	Continuous flow with pump	10–25	76% LPS cell lines 32% LPS serum	125–165	364
Tangential flow filtration	Cancer diagnostics	HeLa Kyoto EGFP-H2B cell line and plasma (ultracentrifuged)	500	50	87	~140	365
Nanowire trapping							
Ciliated porous silicon micropillars	General diagnostics	Mixture of BSA, liposomes and beads	30	10	60% 83 nm liposomes, 15% 120 nm liposomes	80–160	326
Nanowire-embedded PDMS surface microchannel	Bladder and prostate cancer diagnostics	Urine	1,000	50	~99	<200	30
Ciliated anti-CD63 micropillars	Breast cancer diagnostics	Breast cancer cell line MDA-MB-231 (centrifuged)	Continuous flow with pump	10	~75	~100	327
EWI-2 peptide-functionalized ZnO nanowire micropillars	Breast cancer diagnostics	MDA-MB-231 (breast cancer cells) cancer-derived S-EVs	Continuous flow with pump	50	~70	80–160	31
Two-phase precipitation							
Aqueous two-phase serpentine microfluidic system using PEG and DEX	General blood diagnostics	Human plasma (diluted and centrifuged)	10 (continuous flow with a syringe)	2	83.4	40	366
Inertial and viscoelastic flow							
Viscoelasticity-based microfluidic separation of S-EVs	Cancer diagnostics	Adenocarcinoma human alveolar basal epithelial cell isolated S-EVs	Continuous flow with pump	3.3	>80	<200	324
Rapid inertial solution exchange 'RInSE' (CD63 and EpCAM)	Cancer diagnostics (melanoma and breast cancer)	Prepared healthy whole blood and melanoma cell culture and breast cancer cell culture (centrifuged, RBCs lysed and incubated with capture beads and labels)	Continuous flow with pump	70	NA	~30–120	367
'µCENSE' low-speed centrifugal PDMS microfluidic disc	Breast and lung cancer diagnostics	Breast adenocarcinoma cell line MCF-7 and lung adenocarcinoma cell line H1975	15	NA	90	~50–200	368
Wave-like channel, viscoelasticity-based microfluidic separation of S-EVs using poly-(oxyethylene) sheath fluid	Breast cancer diagnostics	MCF-7 and MDA-MB-231 cell culture isolated S-EVs	Continuous sheath flow with pump	25	81	30–200	369
Sequential, waved channel PDMS inertial flow chip	Cancer diagnostics	Nasopharyngeal cancer C666-1 cell-conditioned media	Continuous flow with pump	25	NA	<500	370

ACE, alternating current electrokinetic; BAL, broncheolar lavage; BSA, bovine serum albumin; CTC, circulating tumour cell; DEP, dielectrophoretic; DEX, dextran; DLD, deterministic lateral displacement; ELISA, ELISA, enzyme-linked immunosorbent assay; FIFFF, flow field-flow fractionation; HGSOC, high-grade serous ovarian cancer; iDEP, insulator-based dielectrophoretic; LPS, lipopolysaccharide; NA, not applicable; PDMS, polydimethylsiloxane; PEG, polyethylene glycol; PFP, platelet-free plasma; RBC, red blood cell; S-EV, small extracellular vesicle. [a]Biofluids are of human origin unless otherwise stated.

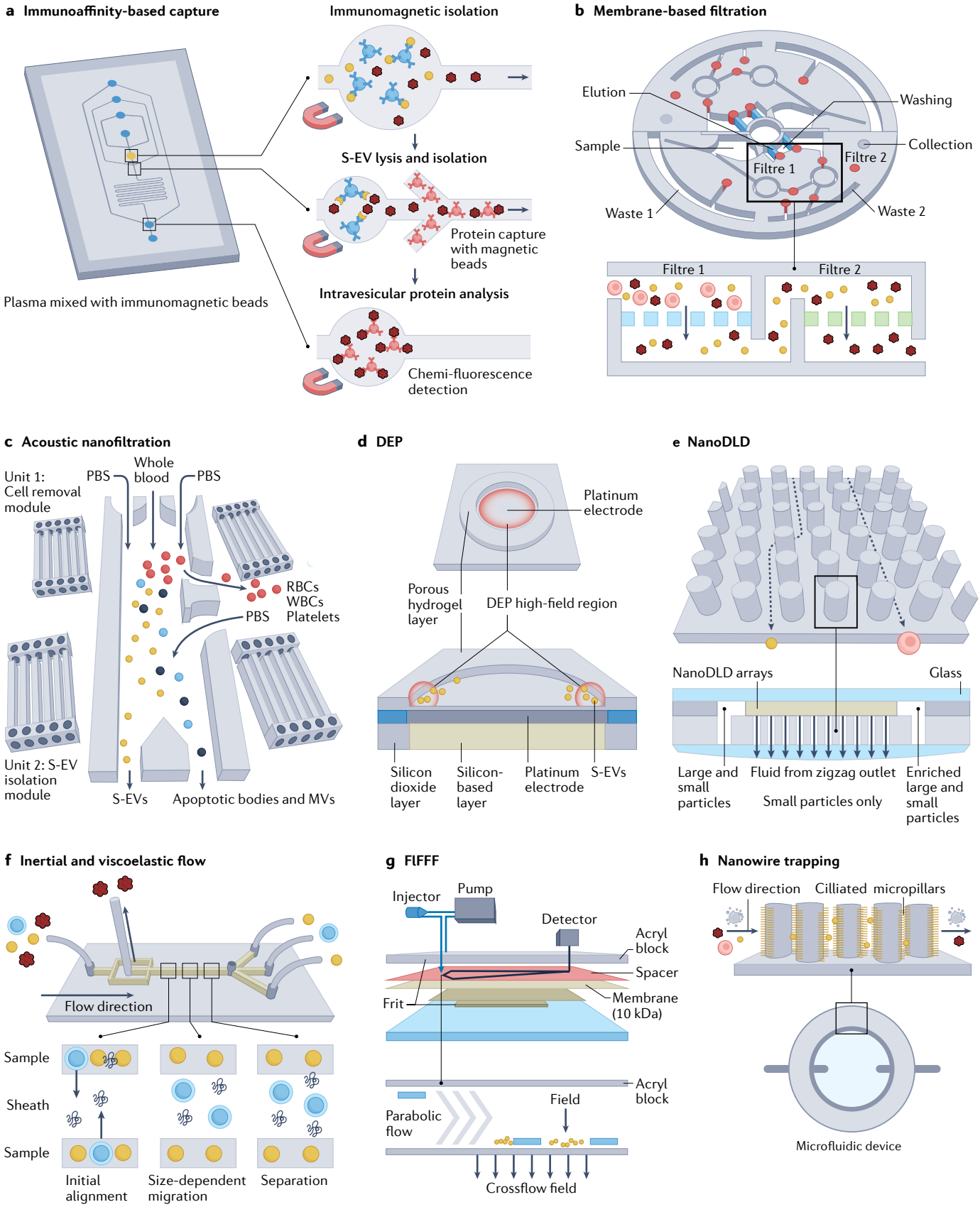
a Immunoaffinity-based capture
Immunomagnetic isolation
Plasma mixed with immunomagnetic beads
S-EV lysis and isolation
Protein capture with magnetic beads
Intravesicular protein analysis
Chemi-fluorescence detection
b Membrane-based filtration
Elution
Washing
Sample
Collection
Filtre 1
Filtre 2
Waste 1
Waste 2
c Acoustic nanofiltration
Unit 1: Cell removal module
PBS
Whole blood
PBS
RBCs
WBCs
Platelets
PBS
Unit 2: S-EV isolation module
S-EVs
Apoptotic bodies and MVs
d DEP
Platinum electrode
Porous hydrogel layer
DEP high-field region
Silicon dioxide layer
Silicon-based layer
Platinum electrode
S-EVs
e NanoDLD
NanoDLD arrays
Glass
Large and small particles
Fluid from zigzag outlet
Small particles only
Enriched large and small particles
f Inertial and viscoelastic flow
Flow direction
Sample
Sheath
Sample
Initial alignment
Size-dependent migration
Separation
g FlFFF
Injector
Pump
Detector
Acryl block
Spacer
Membrane (10 kDa)
Frit
Acryl block
Field
Parabolic flow
Crossflow field
h Nanowire trapping
Flow direction
Cilliated micropillars
Microfluidic device
S-EVs
Large EVs
Immunomagnetic beads
Magnetic beads
PEOs
Cells or large particles
Apoptotic bodies
MVs
Membrane-free soluble proteins
Debris

Fig. 5 | Examples of microfluidic-based methods of S-EV isolation and detection. a, Immunoaffinity-based microfluidic small extracellular vesicles (S-EV) capture[232]. Immunoisolation and on-chip detection of S-EVs using immunomagnetic beads enriched with common S-EV antibodies. **b**, Membrane-based microfluidic filtration[323]. Centrifugal microfluidic platform (Exodisc) using dual membrane filters to isolate S-EVs with a low-speed centrifuge. **c**, Acoustic nanofiltration[312]. Separation of S-EVs using a dual-module 'acoustofluidic' platform with interdigital transducers, creating acoustic waves that discriminate between particle size. **d**, Dielectrophoretic (DEP) microfluidic S-EV isolation[317]. Isolating S-EVs using an alternating current electrokinetic microarray chip, concentrating S-EVs on microelectrodes. **e**, Nano-deterministic lateral displacement (DLD) microfluidic S-EV isolation[35]. A flat channel microfluidic platform with parallel pillar arrays shifted laterally down flow direction to separate particles in a passive flow. **f**, Inertial and viscoelastic flow microfluidic platform[309]. Separation of S-EVs using particle migration behaviour caused by size-dependent elastic lift forces in a viscoelastic medium. **g**, Flow field-flow fractionation (FlFFF) microfluidic S-EV isolation[325]. Fractionation of S-EVs according to hydrodynamic diameter, in which a carrier flow separates particles based on size when met by perpendicular field flow. **h**, Nanowire trapping microfluidic platform[326]. Separation of S-EV-like microvesicles using ciliated silicon nanowires electrodeposited on uniformly arranged micropillars using silver nanoparticle catalysts. EV, extracellular vesicle; MV, microvesicle; PBS, phosphate buffered saline; PEO, poly-(oxyethylene); PLT, platelet; RBC, red blood cell; WBC, white blood cell.

attention, with innovative approaches, such as improving antibody binding and subsequent S-EV capture by bead nanocoating with metal organic frameworks materials to increase surface area[289]. Nanocoating increases antibody immobilization density on the beads and further increases detection resolution of S-EV biomarkers for use in diagnostics. Improving flow cytometry sensitivity and resolution to cater for S-EV size has also been achieved using high-throughput nanoflow cytometry systems such as the Flow Nanoanalyzer (NanoFCM), which operates with high resolution and sensitivity to nanoparticles from 7 to 1,000 nm, also providing comprehensive measurement of particle size, concentration and phenotyping.

Similar to conventional methods, the quantitative and qualitative approaches to analysing S-EVs isolated from microfluidic devices differ greatly between studies. In the majority of studies, total S-EV level measurement, S-EV subgroup differentiation, or intravesicular proteins or mRNA analysis is performed[253]. Several devices integrate two approaches to isolation into a single chip, providing improved outcomes but increasing the complexity of the device. However, these devices display the potential for an integrated platform, functioning as an S-EV isolator, quantifier and analyser.

Immunoaffinity capture microfluidics. Like conventional immunoaffinity-based methods, microfluidic immunoaffinity-based S-EV capture is relatively simple and has high S-EV specificity[256]. S-EV capture methods are based on two fundamental applications of this technique: antibody modification to solid surfaces within the microfluidic channels or capture beads with immobilized antibodies. S-EVs bound on magnetic beads are retained using an external magnetic field, whereas capture beads are commonly magnetic, enabling protein aggregates and other contaminants to be flushed through the device[232]. Antibody binding specificity is unique amongst other methods in that it enables S-EV or EV differentiation amongst heterogenous populations. Immunoaffinity-based and capture-based microfluidic S-EV isolation are by far the most common techniques used, with an abundance of novel platforms having been developed. CD markers are commonly used as targets for specific S-EV immunocapture. These markers (or tetraspanins) are a discrete feature of all S-EVs, irrespective of origin[154]. Importantly, antibodies are not the only affinity-based molecules that can be used to isolate and detect S-EVs, antibody mimetic molecules such as affibodies, have been shown in conventional immunoaffinity isolation to bind with high affinity to S-EV surface proteins[290]. Aptamers also bind effectively to S-EV surface markers and can produce a detectable signal upon S-EV binding, enabling on-chip detection capabilities[90].

Capturing S-EVs on functionalized surfaces requires optimized interaction between as many S-EVs as possible within the biofluid or solution and the surface. A herringbone micromixer structure has been used to considerably improve capture efficiency[270]. This design has subsequently been replicated and improved upon by Dorayappan and colleagues[291]. Y-shaped micropillars were used in two platforms to increase retention time, mixing, and aid in exosome capture[31,273]. The Nano-IMEX platform was created using a graphene oxide and polydopamine nanocoating on these micropillars, which enables improvement of S-EV capture at the 3D-nanostructured interface[273]. Efficiently using antibodies to selectively isolate a target range of surface antigens has been effective in multiple devices based on a functionalized channel surface or capture beads using CD9 (ref.[292]), CD63 (refs.[34,36,293,294]), CD41 (ref.[295]), CD81 (ref.[296]), epidermal growth factor receptor (EGFR)[297], TIM4 (ref.[32]) or multiple markers in conjunction, such as CD24, CD63, EpCAM, FRα, IGF1R, CA125, HER2, MCAM and MCSP[33,232,291,296,298–304] (Table 3).

Alternatively to surface immobilization, functionalized microbeads have also been effective for isolating S-EVs. By mixing functionalized microbeads with S-EVs before sample input, separating, washing and analysing (visualization, characterization and molecular profiling) on chip becomes possible[232,294] (Fig. 5a). The ExoPCD-chip includes an array of Y-shaped micropillars to repetitively cross mix S-EVs and Tim4-modified magnetic microbeads, increasing collisions and, therefore, capture[32]. The Nano-IMEX platform had similar capabilities to the ExoPCD-chip, using enzyme-linked immunosorbent assay (ELISA)-based S-EV detection, showing extremely high sensitivity to targeted S-EVs and an LOD of 50 S-EVs μl^{-1} (ref.[296]). Multiscale integration using a designed self-assembly system has also been developed for the Nano-HB chip, which had a similar herringbone nanopattern with increased surface area for interactions and on-chip detection of CD24-positive, EpCAM-positive and FRα-positive S-EVs at an extremely low LOD of 10 S-EVs μl^{-1}. The ELISA-based μMED platform[282] involves negative labelling of common S-EVs from leukocytes and platelets and positive labelling of target S-EVs to diminish background contamination when analysed using smartphone-based fluorescence detection, resulting in an LOD of 10^4 S-EVs μl^{-1}. The Raman Biochip immunocapture platform is integrated with a Raman detection region using EpCAM-functionalized Raman beads to detect specific S-EVs post CD63-bead capture on-chip[34]. This detection is performed by measuring surface-enhanced Raman scattering peaks, providing a simple method of distinguishing between serum from healthy individuals and serum from patients with prostate cancer. On-chip multiplexed real-time quantitative PCR has been used to identify mRNA content specific to glioblastoma S-EVs[277].

These prototypes display high specificity for S-EVs and require low input volumes, displaying potential for point-of-care diagnostics when integrated with simple methods of characterization and analysis of S-EVs. However, the high specificity for S-EVs has been brought into question, as common S-EV surface markers have been detected on both microvesicle membranes and apoptotic bodies, highlighting the risk of contamination reducing sample purity[305,306]. However, the use of increased flow rates has, in some cases, been detrimental to the capture efficiency and recovery yield of S-EVs[32]. Furthermore, the high cost of S-EV-specific antibodies limits scalability and increases in processing times owing to pre-incubation steps could be improved.

A simplified and rapid ELISA-based method of detecting isolated S-EVs has been proposed, although not yet integrated into microfluidic systems, and provides a simple negative or positive result. This method — lateral flow immunoassay testing or rapid antigen testing — is well established but has only just been applied to isolated cancer S-EVs and consists of a capture antibody (CD81) and detection probe (CD9 conjugated with gold nanoparticles)[307]. Briefly, an S-EV solution is transferred into a microtube containing the detection probe and homogenized, then a nitrocellulose dipstick strip with an anti-tetraspanin antibody test line (T) and an anti-mouse immunoglobulin antibody control line (C) for test verification, is placed into the microtube and allowed to run for 15 min. Unbound AuNP conjugates migrate further to the control line whereas test S-EVs remain on the test line, indicating the presence of the test S-EV population. This test showed a LOD 8.54×10^5 S-EVs/µl for detection with the naked eye. The addition of quantification to this test was attempted using magnetic nanoparticles and an inductive sensor[308]. Using CD63, total EV content was measured, and a targeted S-EV quantification was performed using EVs expressing CD147, a potential colorectal cancer biomarker. This system provided quantification using optical measurements for test line colour intensity from a lateral flow analyser as well as magnetic detection of test lines using a home-made inductive sensor. This technology has the potential for cheap and fast point-of-care diagnostics, but it remains effective only using isolated S-EVs in enriched media and has not been shown to function in minimally processed biofluids, such as seminal plasma after low-speed centrifugation.

Membrane-based filtration microfluidics. Membrane-based filtration in microfluidics is comparable with conventional ultrafiltration, in that nanomembranes are used to isolate particles by movement through pores of a predetermined size[251]. Thus, nanoporous membranes only permit flow of particles smaller than that of the pore size. A microfluidic filtration-based platform has been developed in which either pressure-based filtration or direct-current electrophoresis can be used to isolate S-EVs from mouse whole blood[288]. The pressure-based method clogged the nanopores after extracting only 4 µl of filtrate, whereas the electrophoresis-based isolation negated this issue by removing protein aggregates and resulted in substantially higher recovery of S-EVs with 79.10 (±67.31) ng average RNA per 100 µg protein versus 6.62 (±1.84) ng for the pressure-based method, as well as a higher flow rate of 2 µl min^{-1} versus 0.075 µl min^{-1} for the pressure-based method (Table 3). These outputs required improvement, and dual-filtration platforms have since been developed, such as the Exodisc, which has two integrated nanofilters with low-speed centrifugation to supply flow forces; EVs within the size range of 20–600 nm are isolated using 20-nm pores (Fig. 5b). A dual-nanofilter ExoID-Chip was developed that improved size specificity of EV isolation and integrated detection on the device with photonic crystal nanostructures[290,309]. Size specificity was then further increased using the modular ExoTIC system, which consists of multiple membranes with various pore sizes (200, 100, 50 and 30 nm), enabling connection in sequence for specific size ranges to pass through[291]. This system is simple, fast and has an extremely high yield compared with conventional methods, showing a four-fold higher yield of S-EVs from culture media and up to 1,000-fold higher yield of S-EVs from blood plasma than ultracentrifugation. The ExoSMP has a tri-layer, dual-filtration (100 and 30 nm) and an electrophoretic separation channel[310]. High S-EV recovery (94%) was reported using this device, but cancer cell culture media were used, not highly heterogenous whole blood, serum or plasma.

Filtration alone has a high size specificity but lacks selectivity between S-EV populations or vesicles of similar size[253]. Thus, filtration is better used as an initial isolation step before more selective methods such as immunoaffinity rather than being used as a lone isolation technique. A tri-modular, pneumatically driven, microfluidic platform capable of extremely high S-EV recovery yield (94%) has been developed[258]. S-EVs were isolated from blood using a pressure-driven nanoporous filter with a 200-nm pore size and then enriched with magnetic-bead immunocapture using CD63-antibody-coated microbeads, premixed with S-EVs and fluorescent markers in an on-chip vortex micromixer. Fluorescence was then detected using a photomultiplier tube equipped on a fluorescence microscope. Another pressure-based system has been created that integrates a 200-nm nanoporous filter with a CD63-antibody-functionalized channel[293]; however, a low S-EV recovery yield (32%) from serum of patients with liposarcoma was achieved.

Acoustic isolation microfluidics. Acoustic isolation microfluidics (also known as acoustofluidics) is a size-based method of isolating EVs consisting of acoustic waves that subject varying forces to particles based on their size[311]. A dual-module acoustofluidic filtration platform for whole blood was developed using tilted angle standing surface acoustic waves on each module[294] (Fig. 5c). The initial module removes microscale blood components and cells (red blood cells, white blood cells and platelets), and enriches EVs, whereas the second module separates EVs into S-EVs and other vesicles based on size. This device produced high recovery of S-EVs (82%) and requires no sample pre-processing. Similar prototypes using standing surface acoustic waves to isolate vesicles from conditioned media with blood microvesicles[295] and plasma[294] have also been created. A commercially available AcouTrap instrument (AcouSort AB) was used to trap S-EVs amongst larger seed particles from culture media, urine and plasma using scattered sound particle aggregation[296]. S-EVs are then released once the acoustic wave is turned off.

Acoustofluidics is a new method of microfluidic S-EV isolation and requires further development; the contactless, rapid and label-free properties have the potential for widespread use, but this platform has limited specificity when targeting specific S-EV populations similar to other size-based selection methods such as membrane and inertial microfluidics[311,312].

Dielectrophoretic separation microfluidics. Dielectrophoretic (DEP) separation is based on the dielectric force experienced by particles within a non-uniform electric field[313]. This electric field causes spatial polarization based on particle size and the electrical properties of the surrounding medium. The intensity and frequency of the electric field can be manipulated to alter particle polarization[314–316]. This method has been used in microfluidic separation of S-EVs from undiluted plasma[317]. This device consists of an alternating current electrokinetic microarray using a DEP force to isolate glioblastoma S-EVs in low electric field areas (Fig. 5d). However, this technique suffers from electrothermal heating, which causes reductions in separation ability. Another device, called the ExoDEP chip, integrates immunoaffinity-based capture on microspheres in DEP-based trapping chambers containing pairs of interdigital DEP electrodes, trapping S-EV-bound microspheres with an up to 83% recovery yield from conditioned media[318]. This platform also integrates S-EV detection on-chip and has an extremely low LOD of 193 S-EVs ml^{-1}. Another DEP-based device differed in that the electric field gradient formed at the tip of borosilicate micropipettes and used a relatively low voltage direct current[302]. This design might negate

unintended heating, but improving S-EV isolation purity is difficult with this method when processing complex biofluids. Furthermore, the lack of usability and perceived difficulty in scalability and manufacturability means that this method has limited potential for routine and translatable use.

Deterministic lateral displacement microfluidics. Deterministic lateral displacement (DLD) microfluidic separation consists of an array of micropillars to passively separate S-EVs based on size using a continuous flow through the array[319]. Micropillars are arranged such that the interaction of microparticles with the micropillars can precisely control the trajectory of these particles and isolate particles greater or smaller than a predetermined critical diameter (Dc). The flow path of particles with a diameter greater than the Dc will be altered, whereas particles with a diameter less than the Dc will remain unaffected. Multiple experimental DLD devices have been developed to isolate nanoparticles[319–322]. An important innovation was made by developing a Nanoscale-DLD array in which pillar gap sizes ranged from 25 to 235 nm, enabling targeted isolation of S-EVs between 20 and 100 nm, yet functioned with a very low flow rate of ~0.003 µl min^{-1} owing to the high hydrodynamically resistive features required to isolate exosomes through these arrays[305]. This prototype was improved by integrating >1,000 nanoDLD arrays on a single chip, therefore, increasing the flow rate to 15 µl min^{-1} and S-EVs were isolated from the serum and urine from patients with prostate cancer with a S-EV yield (50%)[35] (Fig. 5e). This improvement in yield is considerable higher than that of a previous DLD-based device reporting a yield of 39%[320], but the yield of other techniques such as membrane filtration (Table 3) is better[278,323]. Microfluidic DLD-based S-EV isolation is often a label-free process; however, reduced S-EV yield and clogging risks reduce the practicality of this technique compared with other methods.

Inertial and viscoelastic flow microfluidics. S-EV isolation using viscoelastic flow is based on the migration patterns of particles in non-Newtonian viscoelastic fluids using inertial properties to isolate S-EVs[324]. A sample fluid containing S-EVs is loaded into a channel with a dynamic sheath flow containing a viscoelastic medium, which subsequently creates an elastic lift force, manipulating and isolating S-EVs and particles in the medium according to size[260]. A viscoelasticity-based microfluidic platform was developed that is capable of separating S-EVs with >80% S-EV recovery at a moderate flow rate of 3.3 µl min^{-1} from conditioned media using a continuous flow of 0.1% poly-(oxyethylene) (PEO) sheath fluid[324]. The isolation of S-EVs <200 nm was set by PEO concentration within the sheath fluid, and this size distribution can be manipulated in increasing or decreasing PEO concentration (Fig. 5f). A similar platform was created that had a wave-like channel structure and a slightly higher PEO concentration (0.16%) and much higher flow rate (25 µl min^{-1})[306]. This platform improves the rate recovery of S-EVs from conditioned media when compared with the previous platform (25 versus 3.3 µl min^{-1}); however, testing on unprocessed, heterogenous biofluids would be a better indication of the efficacy of these approaches than using conditioned media. A simple inertial microfluidic system was designed with a wave-like series of channels with variable thicknesses but low specificity for particles under 500 nm when processing conditioned media[307]. Not inertial microfluidics, but a simple, centrifugal force-based EV separation device called CEntrifugal Nanoparticles Separation and Extraction (mCENSE) has been developed[308]. This device is easy to use but has poor specificity when targeting S-EVs, yet provides a potential platform for downstream integration with other methods to improve specificity.

Integrating inertial microfluidic approaches with other techniques such as immunocapture can improve S-EV specificity, such as with the RInSE platform, in which inertial focussing and buffer exchange enabled flow cytometry analysis with continuous fluorescence detection on-chip with an unreported LOD, and selective immunocapture for more in-depth analysis downstream. Similar to DLD, inertial and viscoelastic flow microfluidic devices suffer from a lack of specificity in S-EV targeting without the use of immunoaffinity binding or more specific size discrimination.

Flow field-flow fractionation microfluidics. Flow field-flow fractionation (FIFFF) microfluidics is an elution-based method of isolating microparticles and nanoparticles from solutions based on size[325]. Isolation occurs using a migration flow in a rectangular channel with an applied secondary crossflow field containing S-EVs. First, this crossflow is applied through a porous channel, creating a diffusion of particles based on size against the wall of the channel causing differential distribution and smaller particles to distribute at a higher mean elevation while larger particles remain lower[325]. The parabolic migration flow is then applied, which removes the smaller particles with a higher mean layer thickness first while larger particles elute last (Fig. 5g). This technique was demonstrated by isolating S-EVs from conditioned culture media using a continuous flow pump, as well as partnering the isolation with liquid chromatography–tandem mass spectrometry[310]. Recovery yield or purity was not reported but the relatively high flow rate would enable samples to be processed in a short time.

Nanowire trapping and filtration microfluidics. Nanowire trapping is the multiscale filtration of particles within a solution based on size and electrostatic interactions, using nanowires coating micropillars and surfaces[326]. This pore-free filtration has the capability to trap S-EVs and vesicles within a particle size range that can be subsequently recovered by elution. A platform with a silicon-ciliated micropillar 'forest' was developed that is capable of capturing liposomes from a conditioned test solution with an input volume of 30 µl and variable recovery yield of 60% using 83 nm liposomes and only 15% using 120 nm liposomes[311] (Fig. 5h). The liposomes were then eluted by dissolving the ciliated nanowires in PBS for 24 h. A ZnO nanowire-coated polydimethylsiloxane surface was created that is able to isolate EVs of S-EV size and morphology without the need for a lengthy elution process[28]. This device had an in situ lysis step for miRNA analysis. This technique was estimated to have a recovery yield of 99% from urine; however, vesicles captured by this method lack specificity.

The purity of S-EV populations captured in nanowire devices can be improved via integration with immunocapture techniques, which have shown improved recovery yields (70–75%) in isolating breast cancer S-EVs[31,327]. This technique has potential owing to the high recovery yield and low run times; however, delicate microstructures require simplification and optimization for capture. The lack of robustness and integrity of these nanofilaments under increased flow rates is a major flaw when compared with more versatile yet less specific systems, such as inertial microfluidics.

Microfluidics is a field in which persisting problems faced by conventional methods, such as starting sample volume, reagents required, time and cost efficiency, and output purity can be addressed. Innovative design and rigorous optimization are required, but the potential for routine use of microfluidics in isolating EVs and S-EVs for clinical use

is now being realized as new technologies are applied to nanoparticle separation and adapted for use in microfluidic devices. The potential for extremely high separation specificity and purity of output samples provides new possibilities for meaningful analysis of targeted populations of S-EVs and, therefore, with further development, providing the possibility of analysing EVs and specifically S-EVs as biomarker carriers.

Idealized diagnostic systems for male infertility

The technology and theoretical basis for an ideal S-EV testing system in male infertility diagnostics might not yet exist, but with microfluidics and increased biomarker research, it could become a reality soon. Hypothetical, idealized systems based on two different approaches have potential in biomarker-based diagnosis of male factor infertility (Fig. 6).

Point-of-need system

A simplified, point-of-need system to identify the levels of three key biomarkers related to sperm dysfunction and subsequent male-factor infertility, which is based on rapid lateral flow immunoassay technology is one potential approach[308] (Fig. 6A). This test should be fast, cheap and user-friendly, centred around point-of-need diagnostics and implemented during sperm isolation within an IVF cycle or during semen analysis for screening. A lateral flow analyser for optical quantification of reads (to prevent user variability for T-line assessment), such as the ESE-Quant LR3 lateral flow system (Qiagen Inc.) is required for a basic output. Isolated seminal plasma would be incubated and homogenized with three types of nanoparticle-conjugated antibodies chosen for biomarker utility (in this case, CRISP1, SPAM1 and MIF). These antibody conjugates and seminal plasma will be transferred to three nitrocellulose strips and placed into a lateral flow reader, which, using optical colour intensity measurements, quantifies increased or reduced levels of each biomarker based on predetermined ranges. For these three potential biomarker examples, low content of CRISP1 and SPAM1 could indicate possibly impaired sperm interaction with the ZP and cumulus cells; thus, ICSI might lead to higher fertilization than conventional IVF. Similarly, increased MIF could indicate impaired sperm motility and increased sperm DFI, prompting ICSI as well as further investigation into sperm DFI analysis.

Multianalyte diagnostics

A multianalyte comprehensive microfluidic-based semen analyser would provide a higher-resolution output of information than a point-of-need system (Fig. 6B). Briefly, a disposable microfluidics chip will be inserted into a specially designed comprehensive semen analyser and reader, which will prime the chip's channels with a buffer and raw semen will be aliquoted directly into the machine at an inlet. Once primed, the machine will then allow the semen to flow into the microfluidic chip inlet (Fig. 6Ba). The sample will flow into a semen analysis chamber in which basic semen parameters, including sperm concentration, motility and sperm morphology, will be assessed using computer-aided semen analysis software (Fig. 6Bb). Simultaneously, a portion of the sample flows through the device along with a dilution buffer through a nanoporous membrane filtration module with 200-nm pores, isolating only S-EVs and proteins (Fig. 6Bc). The semen filtrate then flows into an immunocapture module and binds to a functionalized herringbone surface with S-EV-specific surface marker antibodies CD9, CD63 and CD81 bound with fluorescent reporter antibodies[33] while the protein-containing filtrate is collected and filtered once again to remove any S-EVs or other debris apart from soluble proteins, and is analysed later (Fig. 6Bd). After sufficient S-EV capture has occurred, determined by exosome-bound reporter antibody fluorescence, elution buffer is re-flushed over the functionalized surface to release the captured S-EVs (Fig. 6Be). The eluent is divided and analysed within the device with distinct, clinically relevant outputs (Fig. 6Bf). This approach need not be rapid and could be implemented during follicle stimulation, providing important information relating to sperm functionality and the approach to insemination that would offer the highest rate of success. This improvement in success would be achieved by both replacing current diagnostics for semen and adding multiple molecular predictors of fertilization rates, embryo quality and pregnancy outcome. Soluble proteins, S-EV protein and miRNA panels will be assessed based on predetermined biomarkers of all stages of sperm function. These biomarkers would be used to identify possible impairments in sperm function that are not identified by computer-aided semen analysis. These outputs can provide information to clinicians and scientists to tailor treatments to patients before insemination and embryo creation, further personalizing treatment and possibly elucidating idiopathic infertility.

Future directions

Seminal plasma as a biofluid for liquid biopsies is relatively easy to acquire and store, enabling integration into diagnostic workflows in hospitals, clinics or even homes. The clinical implications of understanding male reproductive S-EV contents and their interaction with sperm in instances of both male and female infertility include the ability to elucidate therapeutic approaches directed by S-EV protein or nucleic acid profiles and provide actionable molecular and mechanistic information for clinicians to tailor ART treatments to a patient's pathophysiology down to a molecular level. However, overcoming the practical limitations of isolating and using S-EVs in diagnostics or therapeutics requires substantial progress.

Protein and miRNA biomarkers might be a step towards refining decisions in treating infertility. For example, identifying protein levels in S-EVs related to poor sperm–ZP binding might indicate improved outcomes by performing ICSI as opposed to IVF, to bypass the interaction between sperm and ZP, therefore, reducing the risk of fertilization failure. This knowledge could reduce time to pregnancy and have major financial and emotional benefits for patients and could be executed by hypothetical idealized systems (Fig. 6). S-EV miRNA has been used to predict the presence of testicular sperm in men with azoospermia[205], which could prevent unnecessary surgery and the associated costs. The potential for S-EV-based therapeutics in ART is also incredible: purified S-EVs from men with normospermia who had undergone vasectomy can improve sperm motility; however, S-EVs purified from men with asthenozoospermia reduce motility[68]. This observation not only shows that seminal plasma S-EVs function independently of seminal plasma and also in the post-ejaculation period, but additionally highlights the feasibility of S-EV supplementation to improve sperm parameters clinically, or S-EVs serving as delivery vehicles for drugs or nutrient molecules ex vivo. The future of S-EVs in drug delivery therapeutics is promising, with technology for the manipulation of target-cell-specific moieties on S-EV membranes improving, as well as integration with therapeutic cargoes and the understanding of biodistribution in the body[234,235]. However, the primary limitations remain in the large-scale isolation of pure populations of S-EVs and efficient storage of these S-EVs for future use.[328]. Currently, microfluidics might not provide the scalability for large-scale S-EV isolation in therapeutics, but the personalized patient-specific diagnostic potential of microfluidic S-EVs cannot be ignored.

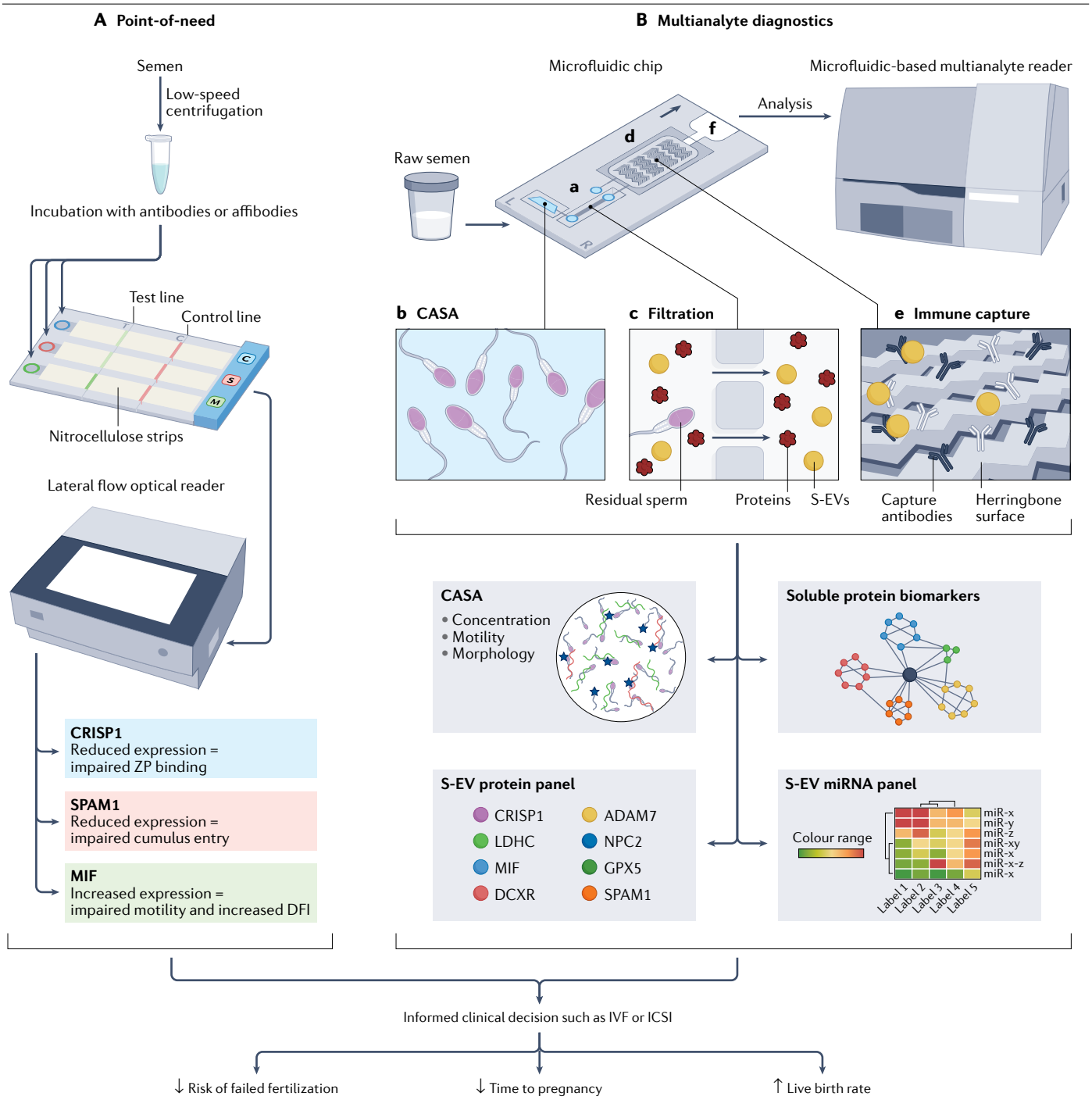

Fig. 6 | Idealized seminal plasma diagnostic systems. A, A point-of-need diagnostic system based on rapid lateral flow immunoassay technology using three proposed seminal plasma biomarkers (CRISP1, SPAM1 and MIF) to determine an insemination approach. **B**, Multianalyte diagnostic microfluidic device and reader using semen analysis, biomarker panel-based proteomics and microRNA (miRNA) analysis to inform clinical decisions based on sperm functionality. **Ba**, Raw semen is loaded into the reader and flows through the loading inlet into a disposable microfluidic chip within the reader. **Bb**, Computer-assisted semen analysis (CASA) assesses semen parameters. **Bc**, Multianalyte reader flows semen through 200-nM nanofilters to isolate small extracellular vesicles (S-EVs) and soluble proteins. **Bd**, S-EV filtrate then flows over an antibody-functionalized herringbone surface and the non-bound proteins are collected for analysis in which the S-EVs are captured on the functionalized surface (part **Be**). **Bf**, Elution buffer flows over the immunocapture module and releases S-EVs from the herringbone surface into the elution tube, which is then analysed with targeted proteomics and miRNA analysis. DFI, DNA fragmentation index; ICSI, intra-cytoplasmic sperm injection; IVF, in vitro fertilization; ZP, zona pellucida.

Overall, four key parameters must be addressed if microfluidics is to be applied in clinical diagnostics in ART: cost effectiveness, usability, reproducibility and accuracy. Devices can often be manufactured on an industrial scale through injection moulding or polymer casting, enabling rapid production once functional and workable devices are developed, or developed around complex multianalyte readers. Supplementary components do increase costs but provide powerful multiplexing capabilities, enabling sorting, detection and analysis on a single platform. The usability of a microfluidics platform relies heavily on the simplicity of the system workflow, and device protocols need to be robust enough to avoid human error. In routine ART, microfluidics-based devices could be integrated into pre-treatment or post-treatment diagnostics to identify underlying molecular causes of infertility. Processing times of even the most laborious and delicate microfluidic devices are still lower than those of conventional methods, although purity and yields vary. The high concentration of seminal plasma S-EVs enables sufficient S-EV output for meaningful analysis even from low-yield devices, provided that purity is high. To create reproducible diagnostic systems, simple operation by non-expert or semi-expert users, combined with consistent flow behaviour of semen or seminal plasma with varying viscosities and densities, is required. Validating these microfluidics devices using analytical methods such as NTA and electron microscopy is simpler once a working product is developed. Medical safety regulatory bodies also require extensive conformity assessments for newly developed medical devices and proof of accuracy with diagnostic devices.

Conclusions

The versatility of S-EV function and variability of their contents highlights the necessity for innovative methods of exploiting these functions while further characterizing proteins and nucleic acids within S-EVs. S-EV function relating to infertility and the associated dysfunctions in human reproductive systems are not fully understood, but these vesicles present a new mode of approaching stagnating success rates within ART and could provide a basis for strong basic science supporting clinically relevant research and ultimately translation. A high demand for novel methods of diagnostics and therapeutics remains, especially when approaching idiopathic infertility, and with further development of microfluidics platforms to integrate routine S-EV isolation and analysis, with proven biomarkers, clinicians can be better informed when approaching arguably ambiguous treatment decisions.

Published online: 08 November 2022

References

1. Arraud, N. et al. Extracellular vesicles from blood plasma: determination of their morphology, size, phenotype and concentration. *J. Thromb. Haemost.* **12**, 614–627 (2014).
2. Pisitkun, T., Shen, R.-F. & Knepper, M. A. Identification and proteomic profiling of exosomes in human urine. *Proc. Natl Acad. Sci. USA* **101**, 13368–13373 (2004).
3. Lässer, C. et al. Human saliva, plasma and breast milk exosomes contain RNA: uptake by macrophages. *J. Transl. Med.* **9**, 1–8 (2011).
4. Emelyanov, A. et al. Cryo-electron microscopy of extracellular vesicles from cerebrospinal fluid. *PLoS ONE* **15**, e0227949 (2020).
5. Vallabhaneni, K. C. et al. Extracellular vesicles from bone marrow mesenchymal stem/stromal cells transport tumor regulatory microRNA, proteins, and metabolites. *Oncotarget* **6**, 4953 (2015).
6. Yáñez-Mó, M. et al. Biological properties of extracellular vesicles and their physiological functions. *J. Extracell. Vesicles* **4**, 27066 (2015).
7. Zaborowski, M. P., Balaj, L., Breakefield, X. O. & Lai, C. P. Extracellular vesicles: composition, biological relevance, and methods of study. *Bioscience* **65**, 783–797 (2015).
8. Deatherage, B. L. & Cookson, B. T. Membrane vesicle release in bacteria, eukaryotes, and archaea: a conserved yet underappreciated aspect of microbial life. *Infect. Immun.* **80**, 1948–1957 (2012).
9. Doyle, L. M. & Wang, M. Z. Overview of extracellular vesicles, their origin, composition, purpose, and methods for exosome isolation and analysis. *Cells* **8**, 727 (2019).
10. Colombo, M., Raposo, G. & Théry, C. Biogenesis, secretion, and intercellular interactions of exosomes and other extracellular vesicles. *Annu. Rev. Cell Dev. Biol.* **30**, 255–289 (2014).
11. Chargaff, E. & West, R. The biological significance of the thromboplastic protein of blood. *J. Biol. Chem.* **166**, 189–197 (1946).
12. Bonucci, E. Fine structure and histochemistry of "calcifying globules" in epiphyseal cartilage. *Z. Zellforsch. Mikroskop. Anat.* **103**, 192–217 (1970).
13. Pegtel, D. M. & Gould, S. J. Exosomes. *Annu. Rev. Biochem.* **88**, 487–514 (2019).
14. Valadi, H. et al. Exosome-mediated transfer of mRNAs and microRNAs is a novel mechanism of genetic exchange between cells. *Nat. Cell Biol.* **9**, 654–659 (2007).
15. Men, Y. et al. Exosome reporter mice reveal the involvement of exosomes in mediating neuron to astroglia communication in the CNS. *Nat. Commun.* **10**, 4136 (2019).
16. Raposo, G. & Stoorvogel, W. Extracellular vesicles: exosomes, microvesicles, and friends. *J. Cell Biol.* **200**, 373–383 (2013).
17. Gurung, S., Perocheau, D., Touramanidou, L. & Baruteau, J. The exosome journey: from biogenesis to uptake and intracellular signalling. *Cell Commun. Signal.* **19**, 47 (2021).
18. Andaloussi, S. E., Mäger, I., Breakefield, X. O. & Wood, M. J. Extracellular vesicles: biology and emerging therapeutic opportunities. *Nat. Rev. Drug Discov.* **12**, 347–357 (2013).
19. Ettelaie, C., Collier, M. E., Maraveyas, A. & Ettelaie, R. Characterization of physical properties of tissue factor-containing microvesicles and a comparison of ultracentrifuge-based recovery procedures. *J. Extracell. Vesicles* **3**, 23592 (2014).
20. Battistelli, M. & Falcieri, E. Apoptotic bodies: particular extracellular vesicles involved in intercellular communication. *Biology* **9**, 21 (2020).
21. Ihara, T., Yamamoto, T., Sugamata, M., Okumura, H. & Ueno, Y. The process of ultrastructural changes from nuclei to apoptotic body. *Virchows Arch.* **433**, 443–447 (1998).
22. Hristov, M., Erl, W., Linder, S. & Weber, P. C. Apoptotic bodies from endothelial cells enhance the number and initiate the differentiation of human endothelial progenitor cells in vitro. *Blood* **104**, 2761–2766 (2004).
23. Elmore, S. Apoptosis: a review of programmed cell death. *Toxicol. Pathol.* **35**, 495–516 (2007).
24. Ronquist, G., Brody, I., Gottfries, A. & Stegmayr, B. An Mg^{2+} and Ca^{2+}-stimulated adenosine triphosphatase in human prostatic fluid — part II. *Andrologia* **10**, 427–433 (1978).
25. Murdica, V. et al. Seminal plasma of men with severe asthenozoospermia contain exosomes that affect spermatozoa motility and capacitation. *Fertil. Steril.* **111**, 897–908. e892 (2019).
26. Lin, Y. et al. Proteomic analysis of seminal extracellular vesicle proteins involved in asthenozoospermia by iTRAQ. *Mol. Reprod. Dev.* **86**, 1094–1105 (2019).
27. Park, K.-H. et al. Ca^{2+} signaling tools acquired from prostasomes are required for progesterone-induced sperm motility. *Sci. Signal.* **4**, ra31 (2011).
28. Aalberts, M. et al. Spermatozoa recruit prostasomes in response to capacitation induction. *Biochim. Biophys. Acta* **1834**, 2326–2335 (2013).
29. Whitesides, G. M. The origins and the future of microfluidics. *Nature* **442**, 368–373 (2006).
30. Yasui, T. et al. Unveiling massive numbers of cancer-related urinary-microRNA candidates via nanowires. *Sci. Adv.* **3**, e1701133 (2017).
31. Suwatthanarak, T. et al. Microfluidic-based capture and release of cancer-derived exosomes via peptide–nanowire hybrid interface. *Lab Chip* **21**, 597–607 (2021).
32. Xu, H., Liao, C., Zuo, P., Liu, Z. & Ye, B. C. Magnetic-based microfluidic device for on-chip isolation and detection of tumor-derived exosomes. *Anal. Chem.* **90**, 13451–13458 (2018).
33. Zhang, P. et al. Ultrasensitive detection of circulating exosomes with a 3D-nanopatterned microfluidic chip. *Nat. Biomed. Eng.* **3**, 438–451 (2019).
34. Kanwar, S. S., Dunlay, C. J., Simeone, D. M. & Nagrath, S. Microfluidic device (ExoChip) for on-chip isolation, quantification and characterization of circulating exosomes. *Lab Chip* **14**, 1891–1900 (2014).
35. Smith, J. T. et al. Integrated nanoscale deterministic lateral displacement arrays for separation of extracellular vesicles from clinically-relevant volumes of biological samples. *Lab Chip* **18**, 3913–3925 (2018).
36. Wang, Y. et al. Microfluidic Raman biochip detection of exosomes: a promising tool for prostate cancer diagnosis. *Lab Chip* **20**, 4632–4637 (2020).
37. Machtinger, R., Laurent, L. C. & Baccarelli, A. A. Extracellular vesicles: roles in gamete maturation, fertilization and embryo implantation. *Hum. Reprod. Update* **22**, 182–193 (2016).
38. Harding, C. V., Heuser, J. E. & Stahl, P. D. Exosomes: looking back three decades and into the future. *J. Cell Biol.* **200**, 367–371 (2013).
39. Zheng, R. et al. Exosome-transmitted long non-coding RNA PTENP1 suppresses bladder cancer progression. *Mol. Cancer* **17**, 1–13 (2018).
40. Zamani, P., Fereydouni, N., Butler, A. E., Navashenaq, J. G. & Sahebkar, A. The therapeutic and diagnostic role of exosomes in cardiovascular diseases. *Trends Cardiovasc. Med.* **29**, 313–323 (2019).
41. Pan, B.-T. & Johnstone, R. M. Fate of the transferrin receptor during maturation of sheep reticulocytes in vitro: selective externalization of the receptor. *Cell* **33**, 967–978 (1983).
42. Cocucci, E., Racchetti, G. & Meldolesi, J. Shedding microvesicles: artefacts no more. *Trends Cell Biol.* **19**, 43–51 (2009).

43. Denzer, K., Kleijmeer, M. J., Heijnen, H. F. G., Stoorvogel, W. & Geuze, H. J. Exosome: from internal vesicle of the multivesicular body to intercellular signaling device. *J. Cell Sci.* **113**, 3365–3374 (2000).
44. Zhang, M., Ouyang, H. & Xia, G. The signal pathway of gonadotrophins-induced mammalian oocyte meiotic resumption. *Mol. Hum. Reprod.* **15**, 399–409 (2009).
45. Momen-Heravi, F. et al. Impact of biofluid viscosity on size and sedimentation efficiency of the isolated microvesicles. *Front. Physiol.* **3**, 162 (2012).
46. Marleau, A. M., Chen, C.-S., Joyce, J. A. & Tullis, R. H. Exosome removal as a therapeutic adjuvant in cancer. *J. Transl. Med.* **10**, 1–12 (2012).
47. Sandfeld-Paulsen, B. et al. Exosomal proteins as diagnostic biomarkers in lung cancer. *J. Thorac. Oncol.* **11**, 1701–1710 (2016).
48. Yuyama, K., Sun, H., Mitsutake, S. & Igarashi, Y. Sphingolipid-modulated exosome secretion promotes clearance of amyloid-β by microglia. *J. Biol. Chem.* **287**, 10977–10989 (2012).
49. Tomlinson, P. R. et al. Identification of distinct circulating exosomes in Parkinson's disease. *Ann. Clin. Transl. Neurol.* **2**, 353–361 (2015).
50. Feng, J., Waqas, A., Zhu, Z. & Chen, L. Exosomes: applications in respiratory infectious diseases and prospects for coronavirus disease 2019 (COVID-19). *J. Biomed. Nanotechnol.* **16**, 399–418 (2020).
51. Nagashima, S. et al. Hepatitis E virus egress depends on the exosomal pathway, with secretory exosomes derived from multivesicular bodies. *J. Gen. Virol.* **95**, 2166–2175 (2014).
52. Martin-DeLeon, P. A. Uterosomes: exosomal cargo during the estrus cycle and interaction with sperm. *Front. Biosci.* **8**, 115–122 (2016).
53. Panner Selvam, M. K., Agarwal, A., Pushparaj, P. N., Baskaran, S. & Bendou, H. Sperm proteome analysis and identification of fertility-associated biomarkers in unexplained male infertility. *Genes* **10**, 522 (2019).
54. Rao, M. et al. Humanin levels in human seminal plasma and spermatozoa are related to sperm quality. *Andrology* **7**, 859–866 (2019).
55. Poliakov, A., Spilman, M., Dokland, T., Amling, C. L. & Mobley, J. A. Structural heterogeneity and protein composition of exosome-like vesicles (prostasomes) in human semen. *Prostate* **69**, 159–167 (2009).
56. Del Giudice, P. T. et al. Determination of testicular function in adolescents with varicocoele — a proteomics approach. *Andrology* **4**, 447–455 (2016).
57. Ronquist, G. & Hedström, M. Restoration of detergent-inactivated adenosine triphosphatase activity of human prostatic fluid with concanavalin A. *Biochim. Biophys. Acta* **483**, 483–486 (1977).
58. Brody, I., Ronquist, G. & Gottfries, A. Ultrastructural localization of the prostasome-an organelle in human seminal plasma. *Ups. J. Med. Sci.* **88**, 63–80 (1983).
59. Ronquist, G. & Brody, I. The prostasome: its secretion and function in man. *Biochim. Biophys. Acta* **822**, 203–218 (1985).
60. Ronquist, G. & Nilsson, B. O. The Janus-faced nature of prostasomes: their pluripotency favours the normal reproductive process and malignant prostate growth. *Prostate Cancer Prostatic Dis.* **7**, 21–31 (2004).
61. Utleg, A. G. et al. Proteomic analysis of human prostasomes. *Prostate* **56**, 150–161 (2003).
62. Stegmayr, B. & Ronquist, G. Promotive effect on human sperm progressive motility by prostasomes. *Urol. Res.* **10**, 253–257 (1982).
63. Thimon, V., Frenette, G., Saez, F., Thabet, M. & Sullivan, R. Protein composition of human epididymosomes collected during surgical vasectomy reversal: a proteomic and genomic approach. *Hum. Reprod.* **23**, 1698–1707 (2008).
64. Sahlén, G. et al. Secretions from seminal vesicles lack characteristic markers for prostasomes. *Ups. J. Med. Sci.* **115**, 107–112 (2010).
65. Le Tortorec, A. et al. From ancient to emerging infections: the odyssey of viruses in the male genital tract. *Physiol. Rev.* **100**, 1349–1414 (2020).
66. Agrawal, Y. & Vanha-Perttula, T. Effect of secretory particles in bovine seminal vesicle secretion on sperm motility and acrosome reaction. *Reproduction* **79**, 409–419 (1987).
67. Zhang, X., Vos, H. R., Tao, W. & Stoorvogel, W. Proteomic profiling of two distinct populations of extracellular vesicles isolated from human seminal plasma. *Int. J. Mol. Sci.* **21**, 7957 (2020).
68. Tauber, P., Zaneveld, L., Propping, D. & Schumacher, G. Components of human split ejaculates. *Reproduction* **43**, 249–267 (1975).
69. Taylor, P. & Kelly, R. 19-HydroxyIated E prostaglandins as the major prostaglandins of human semen. *Nature* **250**, 665–667 (1974).
70. Robert, M. & Gagnon, C. Semenogelin I: a coagulum forming, multifunctional seminal vesicle protein. *Cell. Mol. Life Sci.* **55**, 944–960 (1999).
71. Belleannée, C., Calvo, É., Caballero, J. & Sullivan, R. Epididymosomes convey different repertoires of microRNAs throughout the bovine epididymis. *Biol. Reprod.* **89**, 30 (2013).
72. Conine, C. C., Sun, F., Song, L., Rivera-Pérez, J. A. & Rando, O. J. Small RNAs gained during epididymal transit of sperm are essential for embryonic development in mice. *Dev. Cell* **46**, 470–480. e473 (2018).
73. Grunewald, S., Paasch, U., Glander, H. J. & Anderegg, U. Mature human spermatozoa do not transcribe novel RNA. *Andrologia* **37**, 69–71 (2005).
74. Goodrich, R. J., Anton, E. & Krawetz, S. A. in *Spermatogenesis* (eds Carrell, D. T. & Aston, K.I.) 385–396 (Springer, 2013).
75. Rodriguez-Caro, H. et al. In vitro decidualisation of human endometrial stromal cells is enhanced by seminal fluid extracellular vesicles. *J. Extracell. Vesicles* **8**, 1565262 (2019).
76. Bai, R. et al. Induction of immune-related gene expression by seminal exosomes in the porcine endometrium. *Biochem. Biophys. Res. Commun.* **495**, 1094–1101 (2018).
77. Wang, D. et al. Seminal plasma and seminal plasma exosomes of aged male mice affect early embryo implantation via immunomodulation. *Front. Immunol.* **12**, 723409 (2021).
78. Yanagimachi, R., Kamiguchi, Y., Mikamo, K., Suzuki, F. & Yanagimachi, H. Maturation of spermatozoa in the epididymis of the Chinese hamster. *Am. J. Anat.* **172**, 317–330 (1985).
79. Thimon, V., Koukoui, O., Calvo, E. & Sullivan, R. Region-specific gene expression profiling along the human epididymis. *Mol. Hum. Reprod.* **13**, 691–704 (2007).
80. Frenette, G. & Sullivan, R. Prostasome-like particles are involved in the transfer of P_{25}b from the bovine epididymal fluid to the sperm surface. *Mol. Reprod. Dev.* **59**, 115–121 (2001).
81. Frenette, G., Lessard, C. & Sullivan, R. Selected proteins of "prostasome-like particles" from epididymal cauda fluid are transferred to epididymal caput spermatozoa in bull. *Biol. Reprod.* **67**, 308–313 (2002).
82. Rejraji, H. et al. Lipid remodeling of murine epididymosomes and spermatozoa during epididymal maturation. *Biol. Reprod.* **74**, 1104–1113 (2006).
83. Griffiths, G. S., Galileo, D. S., Reese, K. & Martin-DeLeon, P. A. Investigating the role of murine epididymosomes and uterosomes in GPI-linked protein transfer to sperm using SPAM1 as a model. *Mol. Reprod. Dev.* **75**, 1627–1636 (2008).
84. Ecroyd, H., Sarradin, P., Dacheux, J.-L. & Gatti, J.-L. Compartmentalization of prion isoforms within the reproductive tract of the ram. *Biol. Reprod.* **71**, 993–1001 (2004).
85. Gatti, J.-L. et al. Post-testicular sperm environment and fertility. *Anim. Reprod. Sci.* **82**, 321–339 (2004).
86. Fornes, M., Barbieri, A. & Cavicchia, J. Morphological and enzymatic study of membrane-bound vesicles from the lumen of the rat epididymis. *Andrologia* **27**, 1–5 (1995).
87. Grimalt, P., Bertini, F. & Fornes, M. High-affinity sites for β-D-galactosidase on membrane-bound vesicles isolated from rat epididymal fluid. *Arch. Androl.* **44**, 85–91 (2000).
88. Candenas, L. & Chianese, R. Exosome composition and seminal plasma proteome: a promising source of biomarkers of male infertility. *Int. J. Mol. Sci.* 21 (2020).
89. Johnston, D. S. et al. The mouse epididymal transcriptome: transcriptional profiling of segmental gene expression in the epididymis. *Biol. Reprod.* **73**, 404–413 (2005).
90. Zhou, W., De Iuliis, G. N., Dun, M. D. & Nixon, B. Characteristics of the epididymal luminal environment responsible for sperm maturation and storage. *Front. Endocrinol.* **9**, 59 (2018).
91. Nixon, B. et al. The identification of mouse sperm-surface-associated proteins and characterization of their ability to act as decapacitation factors. *Biol. Reprod.* **74**, 275–287 (2006).
92. Dacheux, J. & Voglmayr, J. Sequence of sperm cell surface differentiation and its relationship to exogenous fluid proteins in the ram epididymis. *Biol. Reprod.* **29**, 1033–1046 (1983).
93. Dacheux, J.-L. et al. Mammalian epididymal proteome. *Mol. Cell. Endocrinol.* **306**, 45–50 (2009).
94. Belleannée, C., Thimon, V. & Sullivan, R. Region-specific gene expression in the epididymis. *Cell Tissue Res.* **349**, 717–731 (2012).
95. Ecroyd, H., Belghazi, M., Dacheux, J.-L. & Gatti, J.-L. The epididymal soluble prion protein forms a high-molecular-mass complex in association with hydrophobic proteins. *Biochem. J.* **392**, 211–219 (2005).
96. Girouard, J., Frenette, G. & Sullivan, R. Comparative proteome and lipid profiles of bovine epididymosomes collected in the intraluminal compartment of the caput and cauda epididymidis. *Int. J. Androl.* **34**, e475–e486 (2011).
97. Nixon, B. et al. Proteomic profiling of mouse epididymosomes reveals their contributions to post-testicular sperm maturation. *Mol. Cell. Proteom.* **18**, S91–S108 (2019).
98. Johnson, A. L. & Howards, S. S. Intratubular hydrostatic pressure in testis and epididymis before and after long-term vasectomy in the guinea pig. *Biol. Reprod. Med.* **58**, 197–210 (2012).
99. Turner, T., Gleavy, J. & Harris, J. Fluid movement in the lumen of the rat epididymis: effect of vasectomy and subsequent vasovasostomy. *J. Androl.* **11**, 422–428 (1990).
100. Dacheux, J.-L. et al. The contribution of proteomics to understanding epididymal maturation of mammalian spermatozoa. *Syst. Biol. Reprod. Med.* **58**, 197–210 (2012).
101. Girouard, J., Frenette, G. & Sullivan, R. Compartmentalization of proteins in epididymosomes coordinates the association of epididymal proteins with the different functional structures of bovine spermatozoa. *Biol. Reprod.* **80**, 965–972 (2009).
102. Zhou, W. et al. Mechanisms of tethering and cargo transfer during epididymosome-sperm interactions. *BMC Biol.* **17**, 35 (2019).
103. Edidin, M. The state of lipid rafts: from model membranes to cells. *Annu. Rev. Biophys. Biomol. Struct.* **32**, 257–283 (2003).
104. Sengupta, P., Baird, B. & Holowka, D. Lipid rafts, fluid/fluid phase separation, and their relevance to plasma membrane structure and function. *Semin. Cell Dev. Biol.* **18**, 583–590 (2007).
105. Aitken, R. J. & De Iuliis, G. N. Origins and consequences of DNA damage in male germ cells. *Reprod. Biomed. Online* **14**, 727–733 (2007).
106. Rooney, I. A., Heuser, J. E. & Atkinson, J. P. GPI-anchored complement regulatory proteins in seminal plasma. An analysis of their physical condition and the mechanisms of their binding to exogenous cells. *J. Clin. Invest.* **97**, 1675–1686 (1996).
107. Sloand, E. M. et al. Correction of the PNH defect by GPI-anchored protein transfer. *Blood* **92**, 4439–4445 (1998).
108. Samanta, L., Parida, R., Dias, T. R. & Agarwal, A. The enigmatic seminal plasma: a proteomics insight from ejaculation to fertilization. *Reprod. Biol. Endocrinol.* **16**, 41 (2018).

109. Caballero, J. N., Frenette, G., Belleannée, C. & Sullivan, R. CD9-positive microvesicles mediate the transfer of molecules to bovine spermatozoa during epididymal maturation. *PLoS ONE* **8**, e65364 (2013).
110. Sullivan, R., Frenette, G. & Girouard, J. Epididymosomes are involved in the acquisition of new sperm proteins during epididymal transit. *Asian J. Androl.* **9**, 483–491 (2007).
111. Sullivan, R. Epididymosomes: a heterogeneous population of microvesicles with multiple functions in sperm maturation and storage. *Asian J. Androl.* **17**, 726 (2015).
112. D'Amours, O. et al. Evidences of biological functions of biliverdin reductase A in the bovine epididymis. *J. Cell. Physiol.* **231**, 1077–1089 (2016).
113. Hu, J. et al. Epididymal cysteine-rich secretory proteins are required for epididymal sperm maturation and optimal sperm function. *Mol. Hum. Reprod.* **24**, 111–122 (2018).
114. Martin-DeLeon, P. A. Epididymal SPAM1 and its impact on sperm function. *Mol. Cell. Endocrinol.* **250**, 114–121 (2006).
115. Eickhoff, R. et al. Influence of macrophage migration inhibitory factor (MIF) on the zinc content and redox state of protein-bound sulphydryl groups in rat sperm: indications for a new role of MIF in sperm maturation. *Mol. Hum. Reprod.* **10**, 605–611 (2004).
116. Saez, F., Frenette, G. & Sullivan, R. Epididymosomes and prostasomes: their roles in posttesticular maturation of the sperm cells. *J. Androl.* **24**, 149–154 (2003).
117. Patel, R. et al. Plasma membrane Ca^{2+}-ATPase 4 in murine epididymis: secretion of splice variants in the luminal fluid and a role in sperm maturation. *Biol. Reprod.* **89**, 1–11 (2013).
118. Sullivan, R. Epididymosomes: role of extracellular microvesicles in sperm maturation. *Front. Biosci.* **8**, 106–114 (2016).
119. Simon, C. et al. Extracellular vesicles in human reproduction in health and disease. *Endocr. Rev.* **39**, 292–332 (2018).
120. Ishijima, S., Okuno, M. & Mohri, H. Zeta potential of human X- and Y-bearing sperm. *Int. J. Androl.* **14**, 340–347 (1991).
121. Cuasnicú, P. S. et al. in *The Epididymis: From Molecules to Clinical Practice* (eds Robaire, B. & Hinton, B. T.) 389–403 (Springer, 2002).
122. Kirchhoff, C. & Hale, G. Cell-to-cell transfer of glycosylphosphatidylinositol-anchored membrane proteins during sperm maturation. *Mol. Hum. Reprod.* **2**, 177–184 (1996).
123. Cooper, T. G. & Yeung, C.-H. in *Sperm Cell: Production, Maturation, Fertilization, Regeneration* (eds De Jonge, C. & Barratt, C.) 72–107 (Cambridge Univ. Press, 2006).
124. Miller, D., Brinkworth, M. & Iles, D. Paternal DNA packaging in spermatozoa: more than the sum of its parts? DNA, histones, protamines and epigenetics. *Reproduction* **139**, 287–301 (2010).
125. Cooper, T. in *Tissue Renin-Angiotensin Systems* (eds Mukhopadhyay, A. K. & Raizada, M. K.) 87–101 (Springer, 1995).
126. Jones, R. Membrane remodelling during sperm maturation in the epididymis. *Oxf. Rev. Reprod. Biol.* **11**, 285–337 (1989).
127. Vickram, A. et al. Seminal exosomes — an important biological marker for various disorders and syndrome in human reproduction. *Saudi J. Biol. Sci.* **28**, 3607–3615 (2021).
128. Llorente, A., de Marco, M. C. & Alonso, M. A. Caveolin-1 and MAL are located on prostasomes secreted by the prostate cancer PC-3 cell line. *J. Cell Sci.* **117**, 5343–5351 (2004).
129. Llorente, A., van Deurs, B. & Sandvig, K. Cholesterol regulates prostasome release from secretory lysosomes in PC-3 human prostate cancer cells. *Eur. J. Cell Biol.* **86**, 405–415 (2007).
130. Aalberts, M., Stout, T. & Stoorvogel, W. Prostasomes: extracellular vesicles from the prostate. *Reproduction* **147**, R1–R14 (2014).
131. Sullivan, R. & Saez, F. Epididymosomes, prostasomes, and liposomes: their roles in mammalian male reproductive physiology. *Reproduction* **146**, R21–R35 (2013).
132. Brouwers, J. F. et al. Distinct lipid compositions of two types of human prostasomes. *Proteomics* **13**, 1660–1666 (2013).
133. Arienti, G., Carlini, E. & Palmerini, C. Fusion of human sperm to prostasomes at acidic pH. *J. Membr. Biol.* **155**, 89–94 (1997).
134. Aalberts, M. et al. Identification of distinct populations of prostasomes that differentially express prostate stem cell antigen, annexin A1, and GLIPR2 in humans. *Biol. Reprod.* **86**, 82–82 (2012).
135. Publicover, S., Harper, C. V. & Barratt, C. $[Ca^{2+}]_i$ signalling in sperm — making the most of what you've got. *Nat. Cell Biol.* **9**, 235–242 (2007).
136. Bailey, J. L. Factors regulating sperm capacitation. *Syst. Biol. Reprod. Med.* **56**, 334–348 (2010).
137. Fraser, L. R. The "switching on" of mammalian spermatozoa: molecular events involved in promotion and regulation of capacitation. *Mol. Reprod. Dev.* **77**, 197–208 (2010).
138. Harrison, R. & Miller, N. cAMP-dependent protein kinase control of plasma membrane lipid architecture in boar sperm. *Mol. Reprod. Dev.* **55**, 220–228 (2000).
139. Pons-Rejraji, H. et al. Prostasomes: inhibitors of capacitation and modulators of cellular signalling in human sperm. *Int. J. Androl.* **34**, 568–580 (2011).
140. García-Rodríguez, A., Gosálvez, J., Agarwal, A., Roy, R. & Johnston, S. DNA damage and repair in human reproductive cells. *Int. J. Mol. Sci.* **20**, 31 (2019).
141. Clark, G. F. & Schust, D. J. Manifestations of immune tolerance in the human female reproductive tract. *Front. Immunol.* **4**, 26 (2013).
142. Vojtech, L. et al. Exosomes in human semen carry a distinctive repertoire of small non-coding RNAs with potential regulatory functions. *Nucleic Acids Res.* **42**, 7290–7304 (2014).
143. Kelly, R. et al. Extracellular organelles (prostasomes) are immunosuppressive components of human semen. *Clin. Exp. Immunol.* **86**, 550–556 (1991).
144. Johansson, M., Bromfield, J. J., Jasper, M. J. & Robertson, S. A. Semen activates the female immune response during early pregnancy in mice. *Immunology* **112**, 290–300 (2004).
145. Robertson, S. A., Guerin, L. R., Moldenhauer, L. M. & Hayball, J. D. Activating T regulatory cells for tolerance in early pregnancy — the contribution of seminal fluid. *J. Reprod. Immunol.* **83**, 109–116 (2009).
146. Malla, B., Zaugg, K., Vassella, E., Aebersold, D. M. & Dal Pra, A. Exosomes and exosomal microRNAs in prostate cancer radiation therapy. *Int. J. Radiat. Oncol. Biol. Phys.* **98**, 982–995 (2017).
147. Yang, C. et al. Comprehensive proteomics analysis of exosomes derived from human seminal plasma. *Andrology* **5**, 1007–1015 (2017).
148. Taylor, D. D. & Gercel-Taylor, C. MicroRNA signatures of tumor-derived exosomes as diagnostic biomarkers of ovarian cancer. *Gynecol. Oncol.* **110**, 13–21 (2008).
149. Milardi, D. et al. Proteomic approach in the identification of fertility pattern in seminal plasma of fertile men. *Fertil. Steril.* **97**, 67–73.e61 (2012).
150. De Lazari, F. L. et al. Seminal plasma proteins and their relationship with sperm motility and morphology in boars. *Andrologia* **51**, e13222 (2019).
151. Gilany, K., Minai-Tehrani, A., Savadi-Shiraz, E., Rezadoost, H. & Lakpour, N. Exploring the human seminal plasma proteome: an unexplored gold mine of biomarker for male infertility and male reproduction disorder. *J. Reprod. Infertil.* **16**, 61 (2015).
152. Vernet, P., Aitken, R. & Drevet, J. Antioxidant strategies in the epididymis. *Mol. Cell. Endocrinol.* **216**, 31–39 (2004).
153. Chabory, E. et al. Epididymis seleno-independent glutathione peroxidase 5 maintains sperm DNA integrity in mice. *J. Clin. Invest.* **119**, 2074–2085 (2009).
154. Buschow, S. I. et al. MHC II in dendritic cells is targeted to lysosomes or T cell-induced exosomes via distinct multivesicular body pathways. *Traffic* **10**, 1528–1542 (2009).
155. Gibbs, G. M. et al. Glioma pathogenesis-related 1-like 1 is testis enriched, dynamically modified, and redistributed during male germ cell maturation and has a potential role in sperm-oocyte binding. *Endocrinology* **151**, 2331–2342 (2010).
156. Ronquist, G. *The Male Role in Pregnancy Loss and Embryo Implantation Failure* (ed. Bronson, R.) 191–209 (Springer, 2015).
157. Tarazona, R. et al. Human prostasomes express CD48 and interfere with NK cell function. *Immunobiology* **216**, 41–46 (2011).
158. Burden, H., Holmes, C., Persad, R. & Whittington, K. Prostasomes — their effects on human male reproduction and fertility. *Hum. Reprod. Update* **12**, 283–292 (2006).
159. Garcia-Rodriguez, A., de la Casa, M., Peinado, H., Gosalvez, J. & Roy, R. Human prostasomes from normozoospermic and non-normozoospermic men show a differential protein expression pattern. *Andrology* **6**, 585–596 (2018).
160. Ernesto, J. I. et al. CRISP1 as a novel CatSper regulator that modulates sperm motility and orientation during fertilization. *J. Cell Biol.* **210**, 1213–1224 (2015).
161. Roberts, K. P. et al. Epididymal secreted protein Crisp-1 and sperm function. *Mol. Cell. Endocrinol.* **250**, 122–127 (2006).
162. Roberts, K. P., Wamstad, J. A., Ensrud, K. M. & Hamilton, D. W. Inhibition of capacitation-associated tyrosine phosphorylation signaling in rat sperm by epididymal protein Crisp-1. *Biol. Reprod.* **69**, 572–581 (2003).
163. Weigel Muñoz, M. et al. Influence of the genetic background on the reproductive phenotype of mice lacking Cysteine-Rich Secretory Protein 1 (CRISP1). *Biol. Reprod.* **99**, 373–383 (2018).
164. Maldera, J. A. et al. Human fertilization: epididymal hCRISP1 mediates sperm–zona pellucida binding through its interaction with ZP3. *Mol. Hum. Reprod.* **20**, 341–349 (2014).
165. Da Ros, V. G. et al. Impaired sperm fertilizing ability in mice lacking Cysteine-RIch Secretory Protein 1 (CRISP1). *Dev. Biol.* **320**, 12–18 (2008).
166. Miki, K. Energy metabolism and sperm function. *Soc. Reprod. Fertil. Suppl.* **65**, 309–325 (2007).
167. Odet, F. et al. Lactate dehydrogenase C and energy metabolism in mouse sperm. *Biol. Reprod.* **85**, 556–564 (2011).
168. Rolland, A. D. et al. Identification of genital tract markers in the human seminal plasma using an integrative genomics approach. *Hum. Reprod.* **28**, 199–209 (2013).
169. Li, S. S.-L. et al. Differential activity and synthesis of lactate dehydrogenase isozymes A (muscle), B (heart), and C (testis) in mouse spermatogenic cells. *Biol. Reprod.* **40**, 173–180 (1989).
170. O'Flaherty, C., Beorlegui, N. & Beconi, M. Lactate dehydrogenase-C4 is involved in heparin-and NADH-dependent bovine sperm capacitation. *Andrologia* **34**, 91–97 (2002).
171. Duan, C. & Goldberg, E. Inhibition of lactate dehydrogenase C4 (LDH-C4) blocks capacitation of mouse sperm in vitro. *Cytogenet. Genome Res.* **103**, 352–359 (2003).
172. Odet, F. et al. Expression of the gene for mouse lactate dehydrogenase C (Ldhc) is required for male fertility. *Biol. Reprod.* **79**, 26–34 (2008).
173. Oddo, M., Calandra, T., Bucala, R. & Meylan, P. R. Macrophage migration inhibitory factor reduces the growth of virulent *Mycobacterium tuberculosis* in human macrophages. *Infect. Immun.* **73**, 3783–3786 (2005).
174. Meinhardt, A. et al. Macrophage migration inhibitory factor production by Leydig cells: evidence for a role in the regulation of testicular function. *Endocrinology* **137**, 5090–5095 (1996).
175. Frenette, G., Lessard, C., Madore, E., Fortier, M. A. & Sullivan, R. Aldose reductase and macrophage migration inhibitory factor are associated with epididymosomes and spermatozoa in the bovine epididymis. *Biol. Reprod.* **69**, 1586–1592 (2003).
176. Huleihel, M. et al. Production of macrophage inhibitory factor (MIF) by primary Sertoli cells; its possible involvement in migration of spermatogonial cells. *J. Cell. Physiol.* **232**, 2869–2877 (2017).
177. Henkel, R., Bittner, J., Weber, R., Hüther, F. & Miska, W. Relevance of zinc in human sperm flagella and its relation to motility. *Fertil. Steril.* **71**, 1138–1143 (1999).

178. Frenette, G., Légaré, C., Saez, F. & Sullivan, R. Macrophage migration inhibitory factor in the human epididymis and semen. *Mol. Hum. Reprod.* **11**, 575–582 (2005).
179. Aljabari, B. et al. Imbalance in seminal fluid MIF indicates male infertility. *Mol. Med.* **13**, 199–202 (2007).
180. Ebert, B., Kisiela, M. & Maser, E. Human DCXR — another 'moonlighting protein' involved in sugar metabolism, carbonyl detoxification, cell adhesion and male fertility? *Biol. Rev.* **90**, 254–278 (2015).
181. Légaré, C., Gaudreault, C., St-Jacques, S. & Sullivan, R. P34H sperm protein is preferentially expressed by the human corpus epididymidis. *Endocrinology* **140**, 3318–3327 (1999).
182. Sullivan, R., Saez, F., Girouard, J. & Frenette, G. Role of exosomes in sperm maturation during the transit along the male reproductive tract. *Blood Cells Mol. Dis.* **35**, 1–10 (2005).
183. Parent, S., Lefievre, L., Brindle, Y. & Sullivan, R. Bull subfertility is associated with low levels of a sperm membrane antigen. *Mol. Reprod. Dev.* **52**, 57–65 (1999).
184. Boué, F. & Sullivan, R. Cases of human infertility are associated with the absence of P34H, an epididymal sperm antigen. *Biol. Reprod.* **54**, 1018–1024 (1996).
185. Frapsauce, C. et al. Proteomic identification of target proteins in normal but nonfertilizing sperm. *Fertil. Steril.* **102**, 372–380 (2014).
186. Sullivan, R., Légaré, C., Villeneuve, M., Foliguet, B. & Bissonnette, F. Levels of P34H, a sperm protein of epididymal origin, as a predictor of conventional in vitro fertilization outcome. *Fertil. Steril.* **85**, 1557–1559 (2006).
187. Moskovtsev, S. I., Jarvi, K., Légaré, C., Sullivan, R. & Mullen, J. B. M. Epididymal P34H protein deficiency in men evaluated for infertility. *Fertil. Steril.* **88**, 1455–1457 (2007).
188. Oh, J. S., Han, C. & Cho, C. ADAM7 is associated with epididymosomes and integrated into sperm plasma membrane. *Mol. Cell* **28**, 441–446 (2009).
189. Han, C. et al. Identification of heat shock protein 5, calnexin and integral membrane protein 2B as Adam7-interacting membrane proteins in mouse sperm. *J. Cell. Physiol.* **226**, 1186–1195 (2011).
190. Légaré, C., Thabet, M., Gatti, J.-L. & Sullivan, R. HE1/NPC2 status in human reproductive tract and ejaculated spermatozoa: consequence of vasectomy. *Mol. Hum. Reprod.* **12**, 461–468 (2006).
191. Busso, D. et al. Spermatozoa from mice deficient in Niemann-Pick disease type C2 (NPC2) protein have defective cholesterol content and reduced in vitro fertilising ability. *Reprod. Fertil. Dev.* **26**, 609–621 (2014).
192. Okamura, N. et al. Molecular cloning and characterization of the epididymis-specific glutathione peroxidase-like protein secreted in the porcine epididymal fluid. *Biochim. Biophys. Acta* **1336**, 99–109 (1997).
193. Légaré, C., Thabet, M., Picard, S. & Sullivan, R. Effect of vasectomy on P34H messenger ribonucleic acid expression along the human excurrent duct: a reflection on the function of the human epididymis. *Biol. Reprod.* **64**, 720–727 (2001).
194. Giacomini, E. et al. Comparative analysis of the seminal plasma proteomes of oligoasthenozoospermic and normozoospermic men. *Reprod. Biomed. Online* **30**, 522–531 (2015).
195. Taylor, A. et al. Epididymal specific, selenium-independent GPX5 protects cells from oxidative stress-induced lipid peroxidation and DNA mutation. *Hum. Reprod.* **28**, 2332–2342 (2013).
196. Noblanc, A. et al. Glutathione peroxidases at work on epididymal spermatozoa: an example of the dual effect of reactive oxygen species on mammalian male fertilizing ability. *J. Androl.* **32**, 641–650 (2011).
197. Rejraji, H., Vernet, P. & Drevet, J. L. R. GPX5 is present in the mouse caput and cauda epididymidis lumen at three different locations. *Mol. Reprod. Dev.* **63**, 96–103 (2002).
198. Barranco, I. et al. Glutathione peroxidase 5 is expressed by the entire pig male genital tract and once in the seminal plasma contributes to sperm survival and in vivo fertility. *PLoS ONE* **11**, e0162958 (2016).
199. Kim, E. et al. Sperm penetration through cumulus mass and zona pellucida. *Int. J. Dev. Biol.* **52**, 677–682 (2004).
200. Baba, D. et al. Mouse sperm lacking cell surface hyaluronidase PH-20 can pass through the layer of cumulus cells and fertilize the egg. *J. Biol. Chem.* **277**, 30310–30314 (2002).
201. Myles, D. G., Hyatt, H. & Primakoff, P. Binding of both acrosome-intact and acrosome-reacted guinea pig sperm to the zona pellucida during in vitro fertilization. *Dev. Biol.* **121**, 559–567 (1987).
202. Primakoff, P., Hyatt, H. & Myles, D. G. A role for the migrating sperm surface antigen PH-20 in guinea pig sperm binding to the egg zona pellucida. *J. Cell Biol.* **101**, 2239–2244 (1985).
203. Reese, K. L. et al. Acidic hyaluronidase activity is present in mouse sperm and is reduced in the absence of SPAM1: evidence for a role for hyaluronidase 3 in mouse and human sperm. *Mol. Reprod. Dev.* **77**, 759–772 (2010).
204. Kimura, M. et al. Functional roles of mouse sperm hyaluronidases, HYAL5 and SPAM1, in fertilization. *Biol. Reprod.* **81**, 939–947 (2009).
205. Honbou, K. et al. The crystal structure of DJ-1, a protein related to male fertility and Parkinson's disease. *J. Biol. Chem.* **278**, 31380–31384 (2003).
206. Junn, E., Jang, W. H., Zhao, X., Jeong, B. S. & Mouradian, M. M. Mitochondrial localization of DJ-1 leads to enhanced neuroprotection. *J. Neurosci. Res.* **87**, 123–129 (2009).
207. An, C.-N. et al. Down-regulation of DJ-1 protein in the ejaculated spermatozoa from Chinese asthenozoospermia patients. *Fertil. Steril.* **96**, 19–23.e12 (2011).
208. Yoshida, K. et al. Immunocytochemical localization of DJ-1 in human male reproductive tissue. *Mol. Reprod. Dev.* **66**, 391–397 (2003).
209. Whyard, T. C., Cheung, W., Sheynkin, Y., Waltzer, W. C. & Hod, Y. Identification of RS as a flagellar and head sperm protein. *Mol. Reprod. Dev.* **55**, 189–196 (2000).
210. Wang, J. et al. Proteomic analysis of seminal plasma from asthenozoospermia patients reveals proteins that affect oxidative stress responses and semen quality. *Asian J. Androl.* **11**, 484–491 (2009).
211. Nishinaga, H. et al. Expression profiles of genes in DJ-1-knockdown and L166P DJ-1 mutant cells. *Neurosci. Lett.* **390**, 54–59 (2005).
212. Pegtel, D. M. et al. Functional delivery of viral miRNAs via exosomes. *Proc. Natl Acad. Sci. USA* **107**, 6328–6333 (2010).
213. Hergenreider, E. et al. Atheroprotective communication between endothelial cells and smooth muscle cells through miRNAs. *Nat. Cell Biol.* **14**, 249–256 (2012).
214. Kalluri, R. & LeBleu, V. S. The biology, function, and biomedical applications of exosomes. *Science* 367 (2020).
215. Ma, J. et al. Testosterone-dependent miR-26a-5p and let-7g-5p act as signaling mediators to regulate sperm apoptosis via targeting PTEN and PMAIP1. *Int. J. Mol. Sci.* **19**, 1233 (2018).
216. Barceló, M., Castells, M., Bassas, L., Vigués, F. & Larriba, S. Semen miRNAs contained in exosomes as non-invasive biomarkers for prostate cancer diagnosis. *Sci. Rep.* **9**, 1–16 (2019).
217. Twenter, H. et al. Transfer of microRNAs from epididymal epithelium to equine spermatozoa. *J. Equine Vet. Sci.* **87**, 102841 (2020).
218. Reilly, J. N. et al. Characterisation of mouse epididymosomes reveals a complex profile of microRNAs and a potential mechanism for modification of the sperm epigenome. *Sci. Rep.* **6**, 31794 (2016).
219. Alshanbayeva, A., Tanwar, D. K., Roszkowski, M., Manuella, F. & Mansuy, I. M. Early life stress affects the miRNA cargo of epididymal extracellular vesicles in mouse. *Biol. Reprod.* **105**, 593–602 (2021).
220. Barcelo, M., Mata, A., Bassas, L. & Larriba, S. Exosomal microRNAs in seminal plasma are markers of the origin of azoospermia and can predict the presence of sperm in testicular tissue. *Hum. Reprod.* **33**, 1087–1098 (2018).
221. Wang, C. et al. Altered profile of seminal plasma microRNAs in the molecular diagnosis of male infertility. *Clin. Chem.* **57**, 1722–1731 (2011).
222. Wu, W. et al. Seminal plasma microRNAs: potential biomarkers for spermatogenesis status. *Mol. Hum. Reprod.* **18**, 489–497 (2012).
223. Abu-Halima, M. et al. Altered micro-ribonucleic acid expression profiles of extracellular microvesicles in the seminal plasma of patients with oligoasthenozoospermia. *Fertil. Steril.* **106**, 1061–1069.e3 (2016).
224. World Health Organization. *Laboratory Manual for the Examination and Processing of Human Semen* 6th edn (WHO, 2021).
225. Santi, D., Spaggiari, G. & Simoni, M. Sperm DNA fragmentation index as a promising predictive tool for male infertility diagnosis and treatment management–meta-analyses. *Reprod. Biomed. Online* **37**, 315–326 (2018).
226. Ferlin, A. et al. Male infertility: role of genetic background. *Reprod. Biomed. Online* **14**, 734–745 (2007).
227. Vashisht, A. & Gahlay, G. K. Using miRNAs as diagnostic biomarkers for male infertility: opportunities and challenges. *Mol. Hum. Reprod.* **26**, 199–214 (2020).
228. Murdica, V. et al. Proteomic analysis reveals the negative modulator of sperm function glycodelin as over-represented in semen exosomes isolated from asthenozoospermic patients. *Hum. Reprod.* **34**, 1416–1427 (2019).
229. Madison, M. N., Roller, R. J. & Okeoma, C. M. Human semen contains exosomes with potent anti-HIV-1 activity. *Retrovirology* **11**, 1–16 (2014).
230. Hiemstra, T. F. et al. Human urinary exosomes as innate immune effectors. *J. Am. Soc. Nephrol.* **25**, 2017–2027 (2014).
231. György, B. et al. Detection and isolation of cell-derived microparticles are compromised by protein complexes resulting from shared biophysical parameters. *Blood J. Am. Soc. Hematol.* **117**, e39–e48 (2011).
232. He, M., Crow, J., Roth, M., Zeng, Y. & Godwin, A. K. Integrated immunoisolation and protein analysis of circulating exosomes using microfluidic technology. *Lab Chip* **14**, 3773–3780 (2014).
233. Muller, L., Hong, C.-S., Stolz, D. B., Watkins, S. C. & Whiteside, T. L. Isolation of biologically-active exosomes from human plasma. *J. Immunol. Methods* **411**, 55–65 (2014).
234. Das, C. K. et al. Exosome as a novel shuttle for delivery of therapeutics across biological barriers. *Mol. Pharm.* **16**, 24–40 (2018).
235. Yamashita, T., Takahashi, Y. & Takakura, Y. Possibility of exosome-based therapeutics and challenges in production of exosomes eligible for therapeutic application. *Biol. Pharm. Bull.* **41**, 835–842 (2018).
236. Théry, C. et al. Minimal information for studies of extracellular vesicles 2018 (MISEV2018): a position statement of the International Society for Extracellular Vesicles and update of the MISEV2014 guidelines. *J. Extracell. Vesicles* **7**, 1535750 (2018).
237. Fedder, J. Nonsperm cells in human semen: with special reference to seminal leukocytes and their possible influence on fertility. *Arch. Androl.* **36**, 41–65 (1996).
238. Soares Martins, T., Catita, J., Martins Rosa, I., O, A. B. D. C. E. S. & Henriques, A. G. Exosome isolation from distinct biofluids using precipitation and column-based approaches. *PLoS ONE* **13**, e0198820 (2018).
239. Lane, R. E., Korbie, D., Anderson, W., Vaidyanathan, R. & Trau, M. Analysis of exosome purification methods using a model liposome system and tunable-resistive pulse sensing. *Sci. Rep.* **5**, 1–7 (2015).
240. Lobb, R. J. et al. Optimized exosome isolation protocol for cell culture supernatant and human plasma. *J. Extracell. Vesicles* **4**, 27031 (2015).
241. Coughlan, C. et al. Exosome isolation by ultracentrifugation and precipitation and techniques for downstream analyses. *Curr. Protoc. Cell Biol.* **88**, e110 (2020).

242. Cao, F. et al. Proteomics comparison of exosomes from serum and plasma between ultracentrifugation and polymer-based precipitation kit methods. *Electrophoresis* **40**, 3092–3098 (2019).
243. Madison, M. N., Welch, J. L. & Okeoma, C. M. Isolation of exosomes from semen for in vitro uptake and HIV-1 infection assays. *Bio Protoc.* **7**, e2216 (2017).
244. Kaddour, H. et al. Proteomics profiling of autologous blood and semen exosomes from HIV-infected and uninfected individuals reveals compositional and functional variabilities. *Mol. Cell. Proteom.* **19**, 78–100 (2020).
245. Welch, J. L., Kaufman, T. M., Stapleton, J. T. & Okeoma, C. M. Semen exosomes inhibit HIV infection and HIV-induced proinflammatory cytokine production independent of the activation state of primary lymphocytes. *FEBS Lett.* **594**, 695–709 (2020).
246. Welch, J. L., Kaddour, H., Schlievert, P. M., Stapleton, J. T. & Okeoma, C. M. Semen exosomes promote transcriptional silencing of HIV-1 by disrupting NF-κB/Sp1/Tat circuitry. *J. Virol.* **92**, e00731–18 (2018).
247. Chang, X. et al. Exosomes from women with preeclampsia induced vascular dysfunction by delivering sFlt (soluble Fms-like tyrosine kinase)-1 and sEng (soluble endoglin) to endothelial cells. *Hypertension* **72**, 1381–1390 (2018).
248. Gemoll, T. et al. Protein profiling of serum extracellular vesicles reveals qualitative and quantitative differences after differential ultracentrifugation and ExoQuick™ isolation. *J. Clin. Med.* **9**, 1429 (2020).
249. Wang, X. in *Extracellular Vesicles* (eds Kuo, W. P. & Jia, S.) 351–353 (Springer, 2017).
250. Yamada, T., Inoshima, Y., Matsuda, T. & Ishiguro, N. Comparison of methods for isolating exosomes from bovine milk. *J. Vet. Med. Sci.*, 12-0032 (2012).
251. Lin, S. et al. Progress in microfluidics-based exosome separation and detection technologies for diagnostic applications. *Small* **16**, e1903916 (2020).
252. Théry, C., Amigorena, S., Raposo, G. & Clayton, A. Isolation and characterization of exosomes from cell culture supernatants and biological fluids. *Curr. Protoc. Cell Biol.* **30**, 3.22. 21–23.22. 29 (2006).
253. Contreras-Naranjo, J. C., Wu, H. J. & Ugaz, V. M. Microfluidics for exosome isolation and analysis: enabling liquid biopsy for personalized medicine. *Lab Chip* **17**, 3558–3577 (2017).
254. Webber, J. & Clayton, A. How pure are your vesicles? *J. Extracell. Vesicles* **2**, 19861 (2013).
255. Vlassov, A. V., Magdaleno, S., Setterquist, R. & Conrad, R. Exosomes: current knowledge of their composition, biological functions, and diagnostic and therapeutic potentials. *Biochim. Biophys. Acta* **1820**, 940–948 (2012).
256. Liga, A., Vliegenthart, A. D., Oosthuyzen, W., Dear, J. W. & Kersaudy-Kerhoas, M. Exosome isolation: a microfluidic road-map. *Lab Chip* **15**, 2388–2394 (2015).
257. Momen-Heravi, F. et al. Current methods for the isolation of extracellular vesicles. *Biol. Chem.* **394**, 1253–1262 (2013).
258. Faruqu, F. N., Xu, L. & Al-Jamal, K. T. Preparation of exosomes for siRNA delivery to cancer cells. *J. Vis. Exp.* **142**, e58814 (2018).
259. Greening, D. W., Xu, R., Ji, H., Tauro, B. J. & Simpson, R. J. in *Proteomic Profiling* (ed. Posch, A.) 179–209 (Springer, 2015).
260. Yang, D. et al. Progress, opportunity, and perspective on exosome isolation-efforts for efficient exosome-based theranostics. *Theranostics* **10**, 3684–3707 (2020).
261. Baranyai, T. et al. Isolation of exosomes from blood plasma: qualitative and quantitative comparison of ultracentrifugation and size exclusion chromatography methods. *PLoS ONE* **10**, e0145686 (2015).
262. Guan, S. et al. Characterization of urinary exosomes purified with size exclusion chromatography and ultracentrifugation. *J. Proteome Res.* **19**, 2217–2225 (2020).
263. Stranska, R. et al. Comparison of membrane affinity-based method with size-exclusion chromatography for isolation of exosome-like vesicles from human plasma. *J. Transl. Med.* **16**, 1–9 (2018).
264. Al Ali, J. et al. TAF1 transcripts and neurofilament light chain as biomarkers for x-linked dystonia-parkinsonism. *Mov. Disord.* **36**, 206–215 (2021).
265. Vandendriessche, C. et al. Importance of extracellular vesicle secretion at the blood–cerebrospinal fluid interface in the pathogenesis of Alzheimer's disease. *Acta Neuropathol. Commun.* **9**, 1–25 (2021).
266. Salarpour, S. et al. Paclitaxel incorporated exosomes derived from glioblastoma cells: comparative study of two loading techniques. *Daru* **27**, 533–539 (2019).
267. Macías, M. et al. Comparison of six commercial serum exosome isolation methods suitable for clinical laboratories. Effect in cytokine analysis. *Clin. Chem. Lab. Med.* **57**, 1539–1545 (2019).
268. Keller, S., Sanderson, M. P., Stoeck, A. & Altevogt, P. Exosomes: from biogenesis and secretion to biological function. *Immunol. Lett.* **107**, 102–108 (2006).
269. Kastelowitz, N. & Yin, H. Exosomes and microvesicles: identification and targeting by particle size and lipid chemical probes. Chembiochem Eur. *J. Chem. Biol.* **15**, 923 (2014).
270. Song, Z. et al. Development of a $CD6_3$ aptamer for efficient cancer immunochemistry and immunoaffinity-based exosome isolation. *Molecules* **25**, 5585 (2020).
271. Zarovni, N. et al. Integrated isolation and quantitative analysis of exosome shuttled proteins and nucleic acids using immunocapture approaches. *Methods* **87**, 46–58 (2015).
272. Alvarez, M. L., Khosroheidari, M., Ravi, R. K. & DiStefano, J. K. Comparison of protein, microRNA, and mRNA yields using different methods of urinary exosome isolation for the discovery of kidney disease biomarkers. *Kidney Int.* **82**, 1024–1032 (2012).
273. Li, P., Kaslan, M., Lee, S. H., Yao, J. & Gao, Z. Progress in exosome isolation techniques. *Theranostics* **7**, 789 (2017).
274. Phan, T. H. et al. New multiscale characterization methodology for effective determination of isolation–structure–function relationship of extracellular vesicles. *Front. Bioeng. Biotechnol.* **9**, 358 (2021).
275. Heinemann, M. L. et al. Benchtop isolation and characterization of functional exosomes by sequential filtration. *J. Chromatogr. A* **1371**, 125–135 (2014).
276. Marsh, S. R., Pridham, K. J., Jourdan, J. & Gourdie, R. G. Novel protocols for scalable production of high quality purified small extracellular vesicles from bovine milk. *Nanotheranostics* **5**, 488–498 (2021).
277. Manz, A., Graber, N. & Widmer, H. Á. Miniaturized total chemical analysis systems: a novel concept for chemical sensing. *Sens. Actuators B Chem.* **1**, 244–248 (1990).
278. Chen, Y.-S., Ma, Y.-D., Chen, C., Shiesh, S.-C. & Lee, G.-B. An integrated microfluidic system for on-chip enrichment and quantification of circulating extracellular vesicles from whole blood. *Lab Chip* **19**, 3305–3315 (2019).
279. Panesar, S. & Neethirajan, S. Microfluidics: rapid diagnosis for breast cancer. *Nanomicro Lett.* **8**, 204–220 (2016).
280. Nosrati, R. et al. Rapid selection of sperm with high DNA integrity. *Lab Chip* **14**, 1142–1150 (2014).
281. Quinn, M. M. et al. Microfluidic sorting selects sperm for clinical use with reduced DNA damage compared to density gradient centrifugation with swim-up in split semen samples. *Hum. Reprod.* **33**, 1388–1393 (2018).
282. Tung, C.-K. et al. Fluid viscoelasticity promotes collective swimming of sperm. *Sci. Rep.* **7**, 1–9 (2017).
283. Vasilescu, S. A. et al. A microfluidic approach to rapid sperm recovery from heterogeneous cell suspensions. *Sci. Rep.* **11**, 7917 (2021).
284. Son, J. et al. Non-motile sperm cell separation using a spiral channel. *Anal. Methods* **7**, 8041–8047 (2015).
285. Son, J., Samuel, R., Gale, B. K., Carrell, D. T. & Hotaling, J. M. Separation of sperm cells from samples containing high concentrations of white blood cells using a spiral channel. *Biomicrofluidics* **11**, 054106 (2017).
286. Roy, T. K. et al. Embryo vitrification using a novel semi-automated closed system yields in vitro outcomes equivalent to the manual Cryotop method. *Hum. Reprod.* **29**, 2431–2438 (2014).
287. Smith, D., Gaffney, E., Blake, J. & Kirkman-Brown, J. Human sperm accumulation near surfaces: a simulation study. *J. Fluid Mech.* **621**, 289–320 (2009).
288. Ramadan, S. et al. Carbon-dot-enhanced graphene field-effect transistors for ultrasensitive detection of exosomes. *ACS Appl. Mater. Interfaces* **13**, 7854–7864 (2021).
289. Zhand, S. et al. Improving capture efficiency of human cancer cell derived exosomes with nanostructured metal organic framework functionalized beads. *Appl. Mater. Today* **23**, 100994 (2021).
290. Sayyadi, N., Zhand, S., Razavi Bazaz, S. & Warkiani, M. E. Affibody functionalized beads for the highly sensitive detection of cancer cell-derived exosomes. *Int. J. Mol. Sci.* **22**, 12014 (2021).
291. Dorayappan, K. D. P. et al. A microfluidic chip enables isolation of exosomes and establishment of their protein profiles and associated signaling pathways in ovarian cancer. *Cancer Res.* **79**, 3503–3513 (2019).
292. Sancho-Albero, M. et al. Isolation of exosomes from whole blood by a new microfluidic device: proof of concept application in the diagnosis and monitoring of pancreatic cancer. *J. Nanobiotechnol.* **18**, 1–15 (2020).
293. Chen, C. et al. Microfluidic isolation and transcriptome analysis of serum microvesicles. *Lab Chip* **10**, 505–511 (2010).
294. Fang, S. et al. Clinical application of a microfluidic chip for immunocapture and quantification of circulating exosomes to assist breast cancer diagnosis and molecular classification. *PLoS ONE* **12**, e0175050 (2017).
295. Ashcroft, B. A. et al. Determination of the size distribution of blood microparticles directly in plasma using atomic force microscopy and microfluidics. *Biomed. Microdevices* **14**, 641–649 (2012).
296. Zhang, P., He, M. & Zeng, Y. Ultrasensitive microfluidic analysis of circulating exosomes using a nanostructured graphene oxide/polydopamine coating. *Lab Chip* **16**, 3033–3042 (2016).
297. Shao, H. et al. Chip-based analysis of exosomal mRNA mediating drug resistance in glioblastoma. *Nat. Commun.* **6**, 6999 (2015).
298. Im, H. et al. Label-free detection and molecular profiling of exosomes with a nano-plasmonic sensor. *Nat. Biotechnol.* **32**, 490–495 (2014).
299. Vaidyanathan, R. et al. Detecting exosomes specifically: a multiplexed device based on alternating current electrohydrodynamic induced nanoshearing. *Anal. Chem.* **86**, 11125–11132 (2014).
300. Zhao, Z., Yang, Y., Zeng, Y. & He, M. A microfluidic ExoSearch chip for multiplexed exosome detection towards blood-based ovarian cancer diagnosis. *Lab Chip* **16**, 489–496 (2016).
301. Sina, A. A. I. et al. Real time and label free profiling of clinically relevant exosomes. *Sci. Rep.* **6**, 1–9 (2016).
302. Ko, J. et al. Smartphone-enabled optofluidic exosome diagnostic for concussion recovery. *Sci. Rep.* **6**, 1–12 (2016).
303. Hisey, C. L., Dorayappan, K. D. P., Cohn, D. E., Selvendiran, K. & Hansford, D. J. Microfluidic affinity separation chip for selective capture and release of label-free ovarian cancer exosomes. *Lab Chip* **18**, 3144–3153 (2018).
304. Kang, Y. T. et al. Dual-isolation and profiling of circulating tumor cells and cancer exosomes from blood samples with melanoma using immunoaffinity-based microfluidic interfaces. *Adv. Sci.* **7**, 2001581 (2020).

305. Tauro, B. J. et al. Two distinct populations of exosomes are released from LIM1863 colon carcinoma cell-derived organoids. *Mol. Cell. Proteom.* **12**, 587–598 (2013).
306. Crescitelli, R. et al. Distinct RNA profiles in subpopulations of extracellular vesicles: apoptotic bodies, microvesicles and exosomes. *J. Extracell. Vesicles* **2**, 20677 (2013).
307. Oliveira-Rodríguez, M. et al. Development of a rapid lateral flow immunoassay test for detection of exosomes previously enriched from cell culture medium and body fluids. *J. Extracell. Vesicles* **5**, 31803 (2016).
308. Moyano, A. et al. Magnetic lateral flow immunoassay for small extracellular vesicles quantification: application to colorectal cancer biomarker detection. *Sensors* **21**, 3756 (2021).
309. Liu, F. et al. The exosome total isolation chip. *ACS Nano* **11**, 10712–10723 (2017).
310. Chen, Z., Yang, Y., Yamaguchi, H., Hung, M.-C. & Kameoka, J. Isolation of cancer-derived extracellular vesicle subpopulations by a size-selective microfluidic platform. *Biomicrofluidics* **14**, 034113 (2020).
311. Wu, M. et al. Acoustofluidic separation of cells and particles. *Microsyst. Nanoeng.* **5**, 1–18 (2019).
312. Wu, M. et al. Isolation of exosomes from whole blood by integrating acoustics and microfluidics. *Proc. Natl Acad. Sci. USA* **114**, 10584–10589 (2017).
313. Jubery, T. Z., Srivastava, S. K. & Dutta, P. Dielectrophoretic separation of bioparticles in microdevices: a review. *Electrophoresis* **35**, 691–713 (2014).
314. Yun, H., Kim, K. & Lee, W. G. Cell manipulation in microfluidics. *Biofabrication* **5**, 022001 (2013).
315. Zhu, H., Lin, X., Su, Y., Dong, H. & Wu, J. Screen-printed microfluidic dielectrophoresis chip for cell separation. *Biosens. Bioelectron.* **63**, 371–378 (2015).
316. Zheng, L., Brody, J. P. & Burke, P. J. Electronic manipulation of DNA, proteins, and nanoparticles for potential circuit assembly. *Biosens. Bioelectron.* **20**, 606–619 (2004).
317. Ibsen, S. D. et al. Rapid isolation and detection of exosomes and associated biomarkers from plasma. *ACS Nano* **11**, 6641–6651 (2017).
318. Zhao, W. et al. Microsphere mediated exosome isolation and ultra-sensitive detection on a dielectrophoresis integrated microfluidic device. *Analyst* **146**, 5962–5972 (2021).
319. Zeming, K. K., Thakor, N. V., Zhang, Y. & Chen, C.-H. Real-time modulated nanoparticle separation with an ultra-large dynamic range. *Lab Chip* **16**, 75–85 (2016).
320. Santana, S. M., Antonyak, M. A., Cerione, R. A. & Kirby, B. J. Microfluidic isolation of cancer-cell-derived microvesicles from hetergeneous extracellular shed vesicle populations. *Biomed. Microdevices* **16**, 869–877 (2014).
321. Tottori, N., Muramoto, Y., Sakai, H. & Nisisako, T. Nanoparticle separation through deterministic lateral displacement arrays in poly (dimethylsiloxane). *J. Chem. Eng. Jpn.* **53**, 414–421 (2020).
322. Calero, V., Garcia-Sanchez, P., Ramos, A. & Morgan, H. Combining DC and AC electric fields with deterministic lateral displacement for micro- and nano-particle separation. *Biomicrofluidics* **13**, 054110 (2019).
323. Woo, H.-K. et al. Exodisc for rapid, size-selective, and efficient isolation and analysis of nanoscale extracellular vesicles from biological samples. *Acs Nano* **11**, 1360–1370 (2017).
324. Liu, C. et al. Field-free isolation of exosomes from extracellular vesicles by microfluidic viscoelastic flows. *ACS Nano* **11**, 6968–6976 (2017).
325. Kang, D., Oh, S., Ahn, S.-M., Lee, B.-H. & Moon, M. H. Proteomic analysis of exosomes from human neural stem cells by flow field-flow fractionation and nanoflow liquid chromatography–tandem mass spectrometry. *J. Proteome Res.* **7**, 3475–3480 (2008).
326. Wang, Z. et al. Ciliated micropillars for the microfluidic-based isolation of nanoscale lipid vesicles. *Lab Chip* **13**, 2879–2882 (2013).
327. Qi, R. et al. Microfluidic device for the analysis of MDR cancerous cell-derived exosomes' response to nanotherapy. *Biomed. Microdevices* **21**, 1–9 (2019).
328. Willis, G. R., Kourembanas, S. & Mitsialis, S. A. Toward exosome-based therapeutics: isolation, heterogeneity, and fit-for-purpose potency. *Front. Cardiovasc. Med.* **4**, 63 (2017).
329. Luo, J. et al. Immunogenicity study of plasmid DNA encoding mouse cysteine-rich secretory protein-1 (mCRISP 1) as a contraceptive vaccine. *Am. J. Reprod. Immunol.* **68**, 47–55 (2012).
330. Batruch, I. et al. Analysis of seminal plasma from patients with non-obstructive azoospermia and identification of candidate biomarkers of male infertility. *J. Proteome Res.* **11**, 1503–1511 (2012).
331. Batruch, I. et al. Proteomic analysis of seminal plasma from normal volunteers and post-vasectomy patients identifies over 2000 proteins and candidate biomarkers of the urogenital system. *J. Proteome Res.* **10**, 941–953 (2011).
332. Tang, H., Duan, C., Bleher, R. & Goldberg, E. Human lactate dehydrogenase A (LDHA) rescues mouse Ldhc-null sperm function. *Biol. Reprod.* **88**, 91–96 (2013).
333. Anahara, R. et al. Deletion of macrophage migration inhibitory factor gene induces down regulation of sex hormones and ultrastructural abnormalities in mouse testes. *Reprod. Toxicol.* **21**, 167–170 (2006).
334. Grzmil, P. et al. Human cyritestin genes (CYRN1 and CYRN2) are non-functional. *Biochem. J.* **357**, 551–556 (2001).
335. Choi, H. et al. Reduced fertility and altered epididymal and sperm integrity in mice lacking ADAM7. *Biol. Reprod.* **93**, 70 (2015).
336. Kim, T. et al. Expression and relationship of male reproductive ADAMs in mouse. *Biol. Reprod.* **74**, 744–750 (2006).
337. Ronquist, G. K. et al. Biochemical characterization of stallion prostasomes and comparison to their human counterparts. *Syst. Biol. Reprod. Med.* **59**, 297–303 (2013).
338. Chotwiwatthanakun, C. et al. Expression of *Penaeus monodon* ortholog of Niemann–Pick type C-2 in the spermatic tract, and its role in sperm cholesterol removal. *Mol. Reprod. Dev.* **83**, 259–270 (2016).
339. Vilagran, I., Castillo-Martín, M., Prieto-Martínez, N., Bonet, S. & Yeste, M. Triosephosphate isomerase (TPI) and epididymal secretory glutathione peroxidase (GPX5) are markers for boar sperm quality. *Anim. Reprod. Sci.* **100**, 22–30 (2016).
340. Zhou, C., Kang, W. & Baba, T. Functional characterization of double-knockout mouse sperm lacking SPAM1 and ACR or SPAM1 and PRSS21 in fertilization. *J. Reprod. Dev.* **58**, 330–337 (2012).
341. Lin, Y., Mahan, K., Lathrop, W. F., Myles, D. G. & Primakoff, P. A hyaluronidase activity of the sperm plasma membrane protein PH-20 enables sperm to penetrate the cumulus cell layer surrounding the egg. *J. Cell Biol.* **125**, 1157–1163 (1994).
342. Primakoff, P. & Myles, D. G. Penetration, adhesion, and fusion in mammalian sperm-egg interaction. *Science* **296**, 2183–2185 (2002).
343. Sun, Y. et al. DJ-1 deficiency causes metabolic abnormality in ornidazole-induced asthenozoospermia. *Reproduction* **160**, 931–941 (2020).
344. Klinefelter, G., Laskey, J., Ferrell, J., Suarez, J. & Roberts, N. Discriminant analysis indicates a single sperm protein (SP22) is predictive of fertility following exposure to epididymal toxicants. *J. Androl.* **18**, 139–150 (1997).
345. Lyu, Y. et al. Human immunodeficiency virus (HIV) infection and use of illicit substances promote secretion of semen exosomes that enhance monocyte adhesion and induce actin reorganization and chemotactic migration. *Cells* **8**, 1027 (2019).
346. Fabiani, R., Johansson, L., Lundkvist, Ö. & Ronquist, G. Enhanced recruitment of motile spermatozoa by prostasome inclusion in swim-up medium. *Hum. Reprod.* **9**, 1485–1489 (1994).
347. Minelli, A., Moroni, M., Martinez, E., Mezzasoma, I. & Ronquist, G. Occurrence of prostasome-like membrane vesicles in equine seminal plasma. *Reproduction* **114**, 237–243 (1998).
348. Carlsson, L. et al. Characteristics of human prostasomes isolated from three different sources. *Prostate* **54**, 322–330 (2003).
349. Ronquist, K. G., Ronquist, G., Larsson, A. & Carlsson, L. Proteomic analysis of prostate cancer metastasis-derived prostasomes. *Anticancer Res.* **30**, 285–290 (2010).
350. Carlsson, L. et al. Association of cystatin C with prostasomes in human seminal plasma. *Int. J. Androl.* **34**, 363–368 (2011).
351. Chevillet, J. R. et al. Quantitative and stoichiometric analysis of the microRNA content of exosomes. *Proc. Natl Acad. Sci. USA* **111**, 14888–14893 (2014).
352. Du, J. et al. Boar seminal plasma exosomes maintain sperm function by infiltrating into the sperm membrane. *Oncotarget* **7**, 58832 (2016).
353. Milutinović, B., Goč, S., Mitić, N., Kosanović, M. & Janković, M. Surface glycans contribute to differences between seminal prostasomes from normozoospermic and oligozoospermic men. *Ups. J. Med. Sci.* **124**, 111–118 (2019).
354. Lee, K., Shao, H., Weissleder, R. & Lee, H. Acoustic purification of extracellular microvesicles. *ACS Nano* **9**, 2321–2327 (2015).
355. Ku, A. et al. Acoustic enrichment of extracellular vesicles from biological fluids. *Anal. Chem.* **90**, 8011–8019 (2018).
356. Wu, M. et al. Separating extracellular vesicles and lipoproteins via acoustofluidics. *Lab Chip* **19**, 1174–1182 (2019).
357. Shi, L. et al. Rapid and label-free isolation of small extracellular vesicles from biofluids utilizing a novel insulator based dielectrophoretic device. *Lab Chip* **19**, 3726–3734 (2019).
358. Wunsch, B. H. et al. Nanoscale lateral displacement arrays for the separation of exosomes and colloids down to 20 nm. *Nat. Nanotechnol.* **11**, 936–940 (2016).
359. Bai, Y. et al. Rapid isolation and multiplexed detection of exosome tumor markers via queued beads combined with quantum dots in a microarray. *Nanomicro Lett.* **11**, 59 (2019).
360. Davies, R. T. et al. Microfluidic filtration system to isolate extracellular vesicles from blood. *Lab Chip* **12**, 5202–5210 (2012).
361. Cho, S. et al. Isolation of extracellular vesicle from blood plasma using electrophoretic migration through porous membrane. *Sens. Actuators B Chem.* **233**, 289–297 (2016).
362. Liang, L.-G. et al. An integrated double-filtration microfluidic device for isolation, enrichment and quantification of urinary extracellular vesicles for detection of bladder cancer. *Sci. Rep.* **7**, 1–10 (2017).
363. Dong, X. et al. Efficient isolation and sensitive quantification of extracellular vesicles based on an integrated ExoID-Chip using photonic crystals. *Lab Chip* **19**, 2897–2904 (2019).
364. Casadei, L. et al. Cross-flow microfiltration for isolation, selective capture and release of liposarcoma extracellular vesicles. *J. Extracell. Vesicles* **10**, e12062 (2021).
365. Han, Z. et al. Highly efficient exosome purification from human plasma by tangential flow filtration based microfluidic chip. *Sens. Actuators B Chem.* **333**, 129563 (2021).
366. Han, B. H. et al. Isolation of extracellular vesicles from small volumes of plasma using a microfluidic aqueous two-phase system. *Lab Chip* **20**, 3552–3559 (2020).

367. Dudani, J. S. et al. Rapid inertial solution exchange for enrichment and flow cytometric detection of microvesicles. *Biomicrofluidics* **9**, 014112 (2015).
368. Yeo, J. C. et al. Label-free extraction of extracellular vesicles using centrifugal microfluidics. *Biomicrofluidics* **12**, 024103 (2018).
369. Zhou, Y., Ma, Z., Tayebi, M. & Ai, Y. Submicron particle focusing and exosome sorting by wavy microchannel structures within viscoelastic fluids. *Anal. Chem.* **91**, 4577–4584 (2019).
370. Teoh, B. Y. et al. Isolation of exosome from the culture medium of nasopharyngeal cancer (NPC) C666-1 cells using inertial based microfluidic channel. *Biomed. Microdevices* **24**, 12 (2022).
371. Linxweiler, J. & Junker, K. Extracellular vesicles in urological malignancies: an update. *Nat. Rev. Urol.* **17**, 11–27 (2020).

Author contributions

D.M.G. researched data for the article. All authors contributed substantially to discussion of the content. D.M.G. wrote the article. D.M.G., S.A.V., D.K.G. and M.E.W. reviewed and/or edited the manuscript before submission.

Competing interests

The authors declare no competing interests.

Additional information

Correspondence should be addressed to David K. Gardner or Majid E. Warkiani.

Peer review information *Nature Reviews Urology* thanks the anonymous reviewer(s) for their contribution to the peer review of this work.